AN ABSTRACT OF THE THESIS OF

Justin K. Anderson for the degree of Master of Science in Forest Science presented on October 22, 2002.

Title: Patterns in Stream Geomorphology and Implications for Hyporheic Exchange Flow

Abstract approved: _____

Steven M. Wondzell

Longitudinal water surface profiles from high-gradient mountain streams provide useful indicators of the relative potential for hyporheic exchange flow in stream reaches with varying morphology. The spacing between slope breaks in step-pool and pool-riffle streams provides a geomorphic scaling metric that indicates how the length of average hyporheic flow paths change throughout the river continuum.

Twelve stream reaches were randomly selected and surveyed in the Lookout Creek basin at the H.J. Andrews Experimental Forest in the western Cascades Mountains of Oregon. Stream reach morphology was examined for patterns that are expressed over a continuum ranging from headwater to mid-order streams that can be predicted from easily measured drainage basin characteristics. Simple and multiple linear regression models were used to predict changes in lateral complexity in stream reaches, and to predict how the general shape of the water

surface profile changes as drainage basin area increases from 0.6 km^2 to 62.3 km^2. Patterns in the lateral complexity of stream reaches were associated with the degree of channel confinement in valley segments, and longitudinal patterns in bed configuration were strongly associated with the position of a stream reach within the river continuum.

Stream reach longitudinal profiles were evaluated to determine how patterns in slope breaks change throughout the portion of the river continuum represented by the study area. Channel units were defined according to slope categories for flat water, steep water, and step units (FLATs, STEEPs and STEPs). A set of regression models was used to predict how slope break spacing and the general shape of the water surface profile change as drainage basin area increases from 0.6 km^2 to 62.3 km^2. Output from these regression equations was tested against independent field data to evaluate model performance. The models generally performed well.

Longitudinal transects of piezometers were installed along the thalweg of a second order, and a third order stream reach. Longitudinal profiles in the piezometer transects were surveyed, and piezometers were used to measure hydraulic head in stream beds. Data were used to test a theoretical model that predicts downwelling where stream profiles are convex, and upwelling where stream profiles are concave. Overall, the shape of the water surface profile explained 38% of the variation in the distribution of hydraulic pressure head in the streambed. Results demonstrated the usefulness of quantifying the magnitude of

concavities and convexities in stream profiles. A metric for expressing the average water surface concavity (AWSC) is proposed. I demonstrated that this metric could be useful for comparing the potential for hyporheic exchange in stream reaches with varying degrees of stream profile roughness. Results showed a decreasing trend in AWSC as drainage basin area increased.

Upwelling and downwelling zones were identified in piezometer transects, and their longitudinal lengths were measured. The lengths of downwelling zones were compared to the spacing between slope breaks in the water surface profile. Average lengths of downwelling zones and FLAT channel slope units increased with increasing basin area at a similar rate, indicating that slope break spacing was a useful indicator for average downwelling zone length.

My results demonstrate that patterns in stream morphology are useful for predicting patterns in hyporheic exchange flow throughout the river continuum. I suggest that the potential for gravity driven exchange flow decreases along the river continuum as AWSC decreases. I also suggest that the frequency of hydrologic exchange between the stream and the hyporheic zone decreases, and that the average length of hyporheic flow paths increase, across the river continuum.

PATTERNS IN STREAM GEOMORPHOLOGY AND IMPLICATIONS FOR HYPORHEIC EXCHANGE FLOW

by
Justin K. Anderson

A THESIS

submitted to

Oregon State University

in partial fulfillment of
the requirements for the
degree of

Master of Science

Presented October 22, 2002
Commencement June 2003

Master of Science thesis of Justin K. Anderson presented on October 22, 2002

APPROVED:

Major Professor, representing Forest Science

Head of the Department of Forest Science

Dean of the Graduate School

I understand that my thesis will become part of the permanent collection of Oregon State University libraries. My signature below authorizes release of my thesis to any reader upon request.

Justin K. Anderson, Author

ACKNOWLEDGEMENTS

I would like to thank Steve Wondzell for intellectual guidance, friendship, and for providing me with the opportunity to work on this project, which has affected my life in many positive ways since May of 2000. I would like to thank Maggie Reeves for her love, encouragement, energy, and youthful spirit. Thanks to Tim Ballard who worked hard, laughed hard, and kayaked hard; to Eric Hedberg, for bringing skill and patience to this project; to Michael Hughes for many laughs in the field (and elsewhere), skill in surveying and mapping, and inspiring insight on stream geomorphology; to Lindsey Treon for her hard work, reliability, and enthusiasm. Thanks again to Maggie Reeves for her endurance, patience, and skill in winter fieldwork. I thank Michael Gooseff for his contributions in the field, and for brainstorming sessions. I thank Roy Haggerty for encouragement towards a better physical understanding. I thank Mom, Dad, Christopher and Morgan for support, encouragement and years worth of teaching me what life is about.

I am also grateful to many other people who have helped make this thesis possible, including Kermit Cromack, Julia Jones, Arne Skaugset, Jeff McDonnel, John Moreau, Fred Swanson Kelly Christiansen, Kevin McGuire, Nick Scheidt, Dan Saboda, Sherri Johnson, Lisa Ganio, Jack Istock, Colden Baxter, Dave Hibbs, Bob Beschta, Justin LaNier, the HJ. Andrews staff, the National Science Foundation, the department of Forest Science office staff, and the Forestry Computing helpdesk.

TABLE OF CONTENTS

LIST OF FIGURES

LIST OF FIGURES (continued)

LIST OF FIGURES (continued)

LIST OF TABLES

LIST OF TABLES (Continued)

PATTERNS IN STREAM GEOMORPHOLOGY AND IMPLICATIONS FOR HYPORHEIC EXCHANGE FLOW

1. INTRODUCTION

1.1. OVERVIEW OF THE HYPORHEIC ZONE

The hyporheic zone is defined as the shallow alluvial aquifer beneath and immediately adjacent to a stream that contains some proportion of stream water (White, 1993). Original use of the term hyporheic is found in the work of Orghidan (Orghidan, 1959; as cited in Dahm and Vallett, 1996), who described the hyporheic zone as the interface between streams and groundwater, and an environment containing new groundwater and a distinctive biota termed the "hyporheos." The word hyporheic derives from the greek words *hypo* for under, and *rheo*, for flow or current (Dahm and Vallet, 1996). Depending on the focus of a particular study, the hyporheic zone has been characterized according to hydrological (Vallett *et al*., 1993; White, 1993), chemical (Triska *et al*., 1989), and

zoological (Orghidan, 1959; Stanford and Ward, 1988) criteria (Brunke and Gonser, 1997).

Hyporheic exchange flow is the process of stream water entering the hyporheic zone, traveling relatively short distances, and returning to the stream. This process supplies water and solutes, including dissolved oxygen and organic carbon, to microorganisms and invertebrates inhabiting the hyporheic zone (Boulton *et al*., 1998). Within the hyporheic zone, microbially mediated chemical reactions, such as nitrogen transformations, are enhanced compared to groundwater or in-stream environments (Harvey and Wagner, 2000). The return of water from the hyporheic zone to the stream supplies limiting nutrients that affect rates of algal primary production, the composition of algal assemblages, and the recovery of stream reaches after disturbance (Vallett *et al*., 1994; Dahm and Vallet, 1996; Wondzell and Swanson, 1996a).

The hyporheic zone provides habitat to a diverse array of aquatic invertebrates (Stanford and Ward, 1988; Boulton *et al*., 1998) including many types of crustaceans, segmented worms, flatworms, rotifers, water mites, and juvenile stages of aquatic insects. These organisms function to process detrital inputs and are part of complex food webs that link hyporheic zones and streams (Dahm and Vallett, 1996). Production of invertebrates in the hyporheic zone can rival or exceed production in the surface waters of streams (Stanford and Ward, 1988). Hyporheic exchange flow has also been shown to be an important factor influencing the success of trout and salmon spawning (Vaux, 1968; Geist and

Dauble, 1998; Torgenesen *et al*.;1999; Baxter and Hauer, 2000). Fish eggs are commonly incubated in the interstitial voids in stream gravels where subsurface flow supplies dissolved oxygen and regulates temperature, providing favorable conditions for eggs and emerging fry (Curry and Noakes, 1995; Dahm and Vallett, 1996; Montgomery *et al*., 1996).

Techniques used to investigate the hyporheic zone, and hyporheic exchange flow include well and piezometer installations, temperature observations, and stream tracer studies. The hydrometric method relies on closely spaced hydraulic head measurements taken from wells and estimates of saturated hydraulic conductivity to compute subsurface water flow. MODFLOW (McDonald and Harbaugh, 1998), a three-dimensional finite difference groundwater flow model, is commonly used in applications of the hydrometric method. Researchers have successfully used MODFLOW to simulate hyporheic exchange flow (Wondzell and Swanson, 1996b; Wroblicky *et al*., 1998; Kasahara and Wondzell, in press). This technique requires a large amount of data that can be difficult to obtain. Other studies have used temperature differences between the stream and the subsurface to delineate boundaries or mixing zones separating different sources of water in the hyporheic zone (Wondzell and Swanson, 1996b; White *et al*, 1987; Malard, *et al*., 1999; Torgenson, 1999). The use of stream tracer studies to investigate hyporheic processes has increased with the development of and availability of models to interpret the results of stream tracer tests (Bencala and Walters, 1983; Runkel, 1988; Hart, 1995). These models provide estimates of the cross-sectional area of a

transient storage zone commonly considered to be the hyporheic zone, exchange rates between the stream and the storage zone, and information about the residence time of water in the storage zone. Limitations of these models include low sensitivity to variability in residence times, inconsistent results across varying rates of stream discharge, and sensitivity to in-stream surface water storage zones (Harvey *et al*., 1996; Kasahara and Wondzell, in press). All investigations on hyporheic exchange flow are limited by a difficulty in obtaining information about the physical characteristics of subsurface aquifer, heterogeneities in aquifer properties, and problems with scaling-up observations from reach-scale studies (Harvey and Wagner, 2000).

1.2. GEOMORPHPIC CONTROLS ON HYPORHEIC EXCHANGE FLOW

Identifying measurable patterns in the geomorphic control of hyporheic exchange flow within the longitudinal continuum of river systems is an important step in scaling estimates of hyporheic exchange flow at the stream-reach scale and beyond, and key to understanding the significance of hyporheic exchange at the basin scale. Recently there has been a call for a better characterization of the important physical and hydrometric properties of stream-catchment systems that determine the characteristics of transport within a hyporheic zone and that can be routinely measured or mapped along greater distances of streams (Bencala, 2000).

Geomorphic control of the physical processes driving hyporheic exchange flow has been well documented. Several studies have focused on the process by which pressure gradients driving convective transport and advective "pumping" through bed sediments is influenced by the shape of bed forms and water surface slope in laboratory flumes, (Thibodeaux and Boyle, 1987; Packman and Brooks 2001) or in natural settings (Savant *et al*., 1987; White *et al*., 1987; Hill, *et al*., 1998). Other studies have focused on subsurface flow associated with steep hydraulic gradients set up by water-surface slope discontinuities in step-pool and pool-riffle channels (Vaux, 1968; Harvey and Bencala, 1993; Morrice, et. al, 1997; Wroblicky, et. al., 1998; Kasahara and Wondzell, in press). These studies have been invaluable in shaping contemporary thought on the process of hyporheic exchange flow. While the previous studies have been largely successful in demonstrating geomorphic control on the process of hyporheic exchange flow, there has been little attempt to use stream geomorphology as a predictor for changes in the relative dominance of the features controlling hyporheic exchange, or changes in the scale of hyporheic flow paths in different locations along the river continuum. Moreover, there has been little attempt to evaluate the reliability and predictive capability imparted by the increasingly well-documented conceptual relation between stream geomorphology and hyporheic exchange flow.

Ecologists and geomorphologists have long sought to identify longitudinal patterns describing stream systems. Vannote *et al* (1980) hypothesized that stream ecosystem attributes are predictable across continuous gradients of physical

variables from headwaters to mouth in what is commonly termed the river continuum. Stanford and Ward (1993) proposed a conceptual framework, the hyporheic corridor, that incorporates channel-aquifer interactions into the river continuum. The hyporheic corridor concept focuses on connectivity between rivers and floodplain aquifers at the reach scale. Alternating bedrock constrained and unconstrained alluvial reaches typical of river systems draining glaciated mountainous catchments are likened to "beads on a string" along the river continuum. Knighton (1984) observed that systematic changes in bed configuration are expected along the longitudinal continuum of a river, from headwater channels with pool-step sequences or poorly developed pools and riffles to better-defined riffle-pool sequences and finally to ripples and dunes in larger order sand-bed streams. Similarly, Montgomery and Buffington (1997) conceptualized a continuum of channel types ranging in the down-valley direction from cascade to step-pool to plane bed to pool riffle to dune-ripple. Other studies have focused more specifically on the patterns and formation of stepped-bed (Grant *et al*., 1990; Lenzi, 2001) and riffle-pool morphologies (Richards, 1976), and empirical relationships between channel width and bed form spacing have been identified (Keller and Melhorn, 1973; Keller, 1978).

The notion that physical variables including bed form pattern, size and spacing vary predictably across the longitudinal river continuum may have important implications for understanding how the process of hyporheic exchange flow is controlled in different geomorphic settings. Longitudinal patterns in the

relative proportions of bed features found in different stream reaches may allow for ranking the importance of these features for controlling hyporheic exchange flow in different portions of a stream basin. Bed form spacing may offer a metric for scaling predictions of hyporheic flow path lengths in different reaches across the longitudinal river continuum. Water surface profile roughness may serve as an indicator of the magnitude of exchange potential between the stream and interstitial water. The goals of this study include identifying useful patterns in stream geomorphology, determining the reliability of a conceptual model predicting the control of upwelling and downwelling by water surface concavity, and strengthening the current understanding of how stream geomorphology affects hyporheic exchange flow in different places along the longitudinal river continuum.

1.3. OBJECTIVES

The objectives of this study are to: 1) Examine stream reach geomorphology for patterns that are expressed over a portion of the river continuum, and that are predictable from easily measured drainage basin characteristics; 2) Develop a model for producing idealized stream reach profiles representing the physical dimensions of streams in different locations along the river continuum; 3) Field test a simplified conceptual model for predicting the vertical motion of water through the stream bed from the shape of the water surface

profile; and 4) Explore the usefulness of a river continuum model for predicting patterns in hyporheic exchange flow. This study focuses on the portion of the river continuum from headwater through mid-order mountain streams. The general hypothesis is that near-surface hyporheic flow path lengths increase predictably across the river continuum in association with predictable increases in bed form spacing. This general hypothesis is approached by testing two specific hypotheses: #1) Changes in the distribution of pressure head in the stream bed are predictable according to the shape of the water surface profile; and #2) The longitudinal length of downwelling zones increases with increasing basin area.

2. METHODS

2.1. STUDY SITE

All stream reaches and piezometer transects described in this study are in the Lookout Creek Basin within the H.J. Andrews Experimental Forest in the western Cascade Mountains of Oregon, USA (Figure 1). Study sites include 12 spatially independent stream reaches (Figure 1; Table 1), two of which were instrumented with piezometers (reach selection is described below under methods). Elevations within the Lookout Creek watershed range from 428 m to 1620 m.

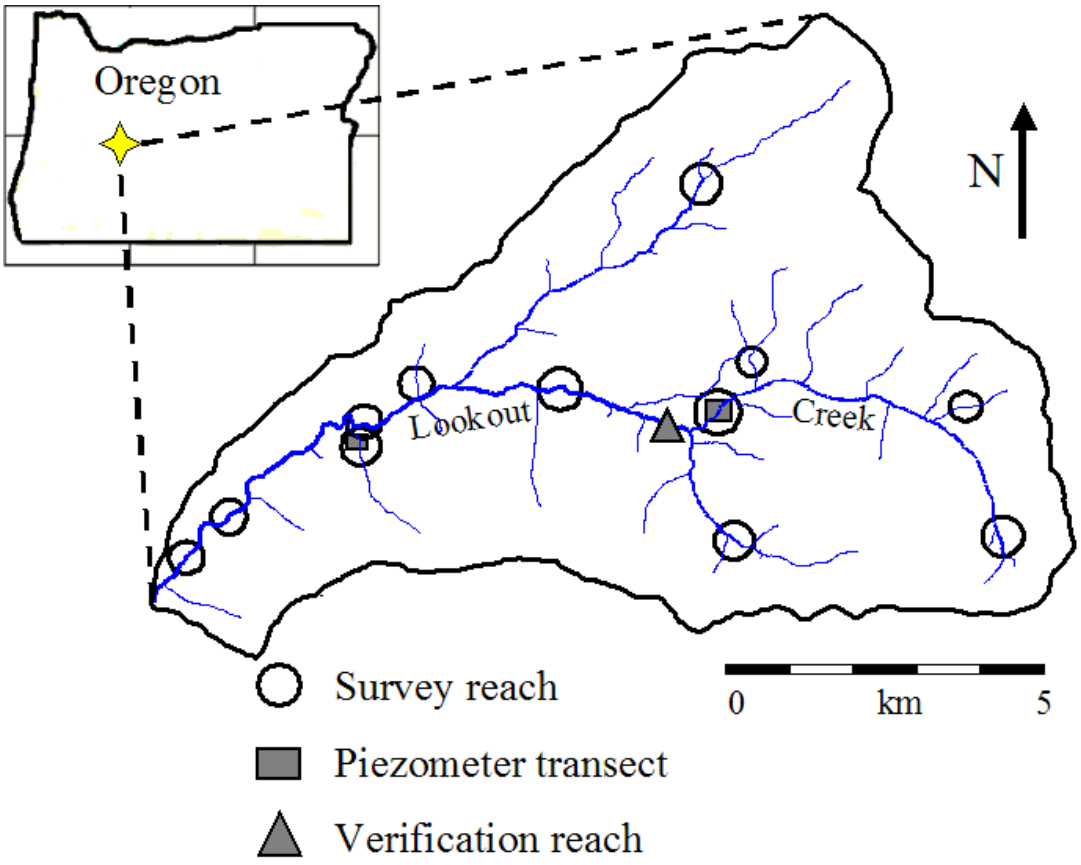

Figure 1: Lookout Creek Basin in the western Cascade Mountains of Oregon, USA.

Average annual precipitation ranges between 2300 mm to 3550 mm and falls mainly between the months of November and March (Bierlmaier and McKee, 1989). Vegetation in the basin consists of coniferous forest dominated by Douglas-fir (*Pseudotsuga menziesii*), western hemlock (*Tsuga beterophylla*), and western redcedar (*Thuja plicata*). Common riparian trees include red alder (*Alnus rubra*) and Scouler willow (*Salix scouleriana*).

Table 1: Stream reach characteristics at study reaches

Stream Reach	Drainage basin area km^2	Average gradient	Valley segment type	Stream reach type
282	0.62	0.202	Alluvial	Cascade
241	1.04	0.078	Alluvial	Step-pool
214	1.12	0.218	Alluvial	Step-pool
395	1.34	0.102	Alluvial	Step-pool
224	1.98	0.102	Alluvial	Step-pool
348	3.85	0.102	Alluvial	Step-pool
333	5.21	0.079	Alluvial	Step-pool
356	16.87	0.048	Alluvial	Step-pool
428	31.29	0.027	Alluvial	Step-pool / Plane bed
416.1 (left channel)	53.86	0.023	Alluvial	Step-pool / Plane bed
416.2 (right channel)	53.86	0.036	Alluvial	Step-pool
407	60.46	0.018	Alluvial/bedrock	Step-pool
403	62.35	0.015	Bedrock	Bedrock

Valley morphology in the Lookout Creek Basin varies from narrow v-shaped valley segments, particularly in headwater catchments, to mid-order valley

segments, some with broad alluvial floodplains. More commonly, mid-order stream segments are constrained by toe slopes, alluvial fans and terraces, and by narrow bedrock gorges lower in the basin (Grant and Swanson, 1995). Based on a channel reach classification system described by Montgomery and Buffington (1997), alluvial stream reach types in the Lookout Creek basin are typically cascade-like or step-pool in the headwaters, and step-pool, or plane bed in mid-order reaches. Bed form shapes are highly irregular due to the presence of wood and boulders. Bed substrates are typically dominated by gravels and cobbles interspersed with boulders.

2.2. FIELD METHODS

2.2.1. Stream reach selection and delineation

The purpose of delineating stream reaches was to identify similar physical units for sampling. An Arcview shapefile of second-, third- and fourth-order (Strahler, 1964) stream segments in the study area was created using a 10-meter digital elevation model (DEM). In this stream layer Lookout Creek is 4^{th} order at its mouth.

Four stream reaches from each order were chosen at random to allow inferences to the entire basin. A computer model was used to systematically

generate UTM coordinates for a population of possible stream reach locations in streams of each order. Locations were numbered and a subset of them was randomly selected for sampling. Stream reach locations were located in the field by using a hand held GPS unit to locate UTM coordinates obtained from the digital map of the study area. Selected locations were treated as the upstream end of a study reach. The downstream ends of reaches were set equal to a distance of 20 active channel widths from the head of the reach. Watershed area at the head of each reach was also calculated from the DEM. One of the randomly selected fourth-order reaches had an island that split the stream in two for the entire reach length. Both channels were surveyed and included in the analysis as separate reaches, where appropriate. This was justified because the separate channels had an overall different character, did not rejoin within the length cutoff of twenty bankful widths, were nearly identical in flow, and were separated in places by islands that were elevated above the active floodplain.

2.2.2. Stream survey methods

Stream reaches were surveyed with an autolevel and a leveling rod between June and August of 2000 and 2001. A fiberglass measuring tape was stretched between stakes driven into the streambed along the thalweg. Streambed elevations and water surface elevations, relative to an arbitrary benchmark, were surveyed at

points along the measuring tape. Survey points were spaced between 0.5 and 8 meters to according to stream feature sizes. This approach allowed us to efficiently capture all channel spanning slope breaks in the stream bed and stream water surface. I used definitions from Schumm (1977) as a guide for defining floodplain features and measuring floodplain and channel widths. Accordingly, the active channel was defined as the part of the floodplain that undergoes active erosion and deposition. The active width was identified by the break between bare, recently scoured alluvium and surfaces either occupied by perennial vegetation or elevated enough to have escaped recent scouring. The confined width was measured as the width of the active floodplain between the lowest terrace level, or valley wall, which ever was nearer the channel. Wetted stream channel widths, and active widths were measured at 10 meter intervals for second order streams, and at 15 meter intervals for third and fourth order streams.

The frequency of side channels and bar-formed secondary channels was recorded for each stream reach. Side channels are defined as extensions of the main channel that are separated by islands that are outside the active channel width (i.e. high enough to avoid periodic flooding). Bar-formed secondary channels include channel splits and alcoves. Channel splits are defined as extensions of the channel that are connected to the main channel at their head, but are separated by bars that occur within the active width of the stream. Channel splits may or may not be connected to the main channel at their tails by surface water. Alcoves are

slack water channels separated from the main channel by bars; they exist in scoured bed depression connected to the main channel at the downstream end.

2.2.3. Defining slope breaks and channel slope units

Longitudinal profiles of water surface elevations were systematically broken into line segments defined by each consecutive pair of survey points. Slope (gradient) was calculated for each line segment as ($\Delta z / \Delta x$), where Δz is a vertical distance, and Δx is a distance along the axis of stream flow. Each line segment was then assigned to one of three categories: FLAT (flat water units--slope <0.025), STEEP (steep water units--0.025 <slope <0.13), or STEP (step units--slope >0.13). Often times, two or more adjacent line segments fell in the same slope category. Collections of consecutive line segments of the same slope category define a Channel Slope Unit (CSU). These are categorized as FLAT, STEEP, or STEP according to the line segments slope criteria (Table 2). Length and slope were calculated for every CSU. FLATs included what are commonly referred to as pools, runs, and glides; STEEPs included riffles and rapids; and STEPs included steps and cascades. Several values for slope categories were tested and compared, but the ones reported yielded CSUs that most closely matched the pattern of pools, riffles and steps observed in the field. Using these slope break categories, average slopes were 0.35% for FLATs, 6.56% for STEEPs, and 37.71% for STEPs.

Table 2: Definitions of some important stream characteristics measured and predicted for this study

Parameter	Abbreviation	Definition
Drainage area	AREA	Source area at head of stream reach
Stream reach gradient	GRAD	TOT.height / TOT.length
Channel Slope Unit	CSU	A distinct unit in the long. profile of a stream reach defined by the slope of the water surface
Flat Water Unit	FLAT	Water surface slope < 0.025
Steep Water Unit	STEEP	0.025<=water surface slope=<0.13
Step Unit	STEP	Water surface slope > 0.13
Median distance between STEPs	Dist.btwn.STEPS	Longitudinal distance from the bottom of one step to the bottom of next
Percent of reach length in FLATs	%FLAT.length	(Sum of the longitudinal lengths of all FLATs / longitudinal length of stream reach) * 100
Percent of reach length in STEEPs	%STEEP.length	(Sum of the longitudinal lengths of all STEEPs / longitudinal length of stream reach) * 100
Percent of reach length in STEPs	%STEP.length	(Sum of the longitudinal lengths of all STEPs / longitudinal length of stream reach) * 100
Percent of reach height in FLATs	%FLAT.height	(Sum of the vertical heights of all FLATs / total vertical height of stream reach) * 100
Percent of reach height in STEEPs	%STEEP.height	(Sum of the vertical heights of all STEEPs / total vertical height of stream reach) * 100
Percent of reach height in STEPs	%STEP.height	(Sum of the vertical heights of all STEPs / total vertical height of stream reach) * 100

2.2.4. Piezometer installation and monitoring

Piezometers were installed in the winter of 2001—2002 in a second order, and a third order stream reach, draining watershed areas of 1.98 km^2, and 16.87 km^2, respectively, representing different positions within the river continuum (Table 3). Piezometer transects were installed longitudinally along the thalweg of the stream in portions of stream reaches with varying morphology. Two separate

longitudinal piezometer transects, (P224.0 and P224.1), were installed nearly adjacently in sequential lengths of a second order reach. Transect P224.0 has 22 piezometers covering a weakly developed step-pool morphology. Just downstream, transect P224.1 has 18 piezometers covering a well-developed step-pool morphology. A single transect of 35 piezometers, (P356.0), was installed in a third order reach, also with a step-pool morphology.

Table 3: Stream reach characteristics within piezometer transects

Piezometer transect	Number of piezometers	Stream order	Drainage basin area (km^2)	Average gradient over transect	Active channel width (m)	Substrates
P224.0	22	2	1.98	5.7%	3.9	Gravels, cobbles, small boulders
P224.1	18	2	1.98	13.%	3.9	Gravels, cobbles, small boulders
P356.0	35	3	16.87	4.8%	9.4	Gravels, cobbles, small boulders

Piezometers were constructed from 1.875 cm inside diameter thin-walled aluminum tubing cut to 90 cm, 120 cm, and 150 cm lengths. Piezometers were screened by drilling 0.24 cm diameter holes spaced 1 cm apart over an interval between 2 and 4 centimeters from the bottom end. The bottom end was crimped to facilitate driving with a sledge hammer and prevent clogging by sediment. Piezometers were installed vertically, 34 cm into the bed (deeper installation was

impractical with this design and these methods). Piezometers were spaced at 1-meter intervals, in longitudinal transects that followed the thalweg of the stream. Depth and spacing were not exact where boulders hindered installation. The relative elevations of the top of each piezometer were surveyed using an auto level and leveling rod. Stream water elevations were calculated as the elevation at the top of the piezometer minus the length of the portion of piezometer protruding above the water surface. Water height in piezometers was measured with a graduated electrical contact meter. Pressure head in piezometers was calculated by subtracting the elevation at the point of the piezometer from the total head measured in the piezometer. Vertical hydraulic gradients were calculated as

$$VHG = \Delta h / \Delta l, \qquad (1)$$

where (Δh) is the elevation of water in the piezometer minus the elevation of the stream water surface, and (Δl) is the distance between the top of the screened interval to the surface of the stream bed. Positive numbers indicate upwelling, whereas negative numbers indicate downwelling. Downwelling zone lengths were defined as the longitudinal distance from the last upwelling piezometer in a series to the last downwelling piezometer in a series of consecutive piezometers.

Water elevations in piezometer transect P356.0 were measured on February 22nd, 2002, at flow conditions that approximated steady winter baseflow. Piezometer transects P224.0 and P224.1 were measured on April 7th, 2002, also at flow conditions near steady winter baseflow. All piezometers were installed at least a week before measuring water elevations. After measuring water elevations,

qualitative tests were performed on piezometers to ensure hydrologic connectivity with the hyporheic zone. Piezometers were filled with water and allowed to re-equilibrate. Five piezometers showed no response over a two hour period and were not used in this analysis.

2.3. THEORETICAL MODEL AND APPLICATION

2.3.1. Derivation of hypothesis #1

The theoretical model described here is not intended to be a comprehensive explanation of physical hydrology in the hyporheic zone. Rather, this model provides a tool for investigating the geomorphic control of hyporheic exchange flow. Vaux (1968) defined the contemporary theoretical model of how stream bed shape influences the flow of water through stream beds by showing that downwelling occurs where the stream profile is convex, and that upwelling occurs where the stream profile is concave. To do this, Vaux (1968) solved the LaPlace equation in two dimensions for selected boundary conditions representing convex and concave stream beds. The shape of the flow net describing the head distribution in the subsurface aquifer is affected by the physical characteristics of the aquifer, including the cross-sectional area, the shape of the underlying

impermeable boundary, and heterogeneities in hydraulic conductivity in the bed sediments.

For steady-state flows in a homogeneous and isotropic aquifer, the two-dimensional form of the LaPlace equation is written as:

$$(\partial^2 H/\partial x^2) + (\partial^2 H/\partial z^2) = 0, \qquad (2)$$

where (H) is the total head, (x) is the longitudinal distance in the downstream direction, and (z) is the elevation above an arbitrary datum. Equation (2) describes the total potential at all points within a two-dimensional flow field. Meaningful solutions to the LaPlace equation require that the boundaries of the aquifer be defined. Vaux assumed an aquifer with an infinite length, meaning that only the upper and lower boundaries of the flow field needed to be defined. Both the aquifer and the stream were assumed to have a constant depth. The upper boundary was defined by the interface between the stream and the stream bed. This was a permeable boundary across which exchange flow was allowed. The lower boundary was defined as a curve exactly parallel to the upper boundary, and was defined as impermeable to represent a bedrock surface beneath the stream bed aquifer. It was assumed that vertical hydraulic gradients could vary in the longitudinal direction, but not in the horizontal or vertical directions. Based on this assumption, the total head distribution in the x-dimension in the potential field described by equation (2) is given by,

$$(d^2H/dx^2) = 0 \qquad (3)$$

In developing a mathematical statement of hypothesis #1, the term (d^2H/dx^2) is broken into gravitational head (given by the elevation, z) and pressure head (P), yielding

$$(d^2z/dx^2) + (d^2P/dx^2) = 0 \qquad (4)$$

Rearranging yields

$$(d^2P/dx^2) = - (d^2z/dx^2) \qquad (5)$$

Equation (5) is a mathematical statement of hypothesis #1. This equation defines the relationship between the distributions of gravitational head and pressure head along a curve within the stream bed that is parallel to the water surface profile. Because the upper and lower boundaries of the theoretical model are parallel, the term (d^2z/dx^2) is equal for any curve parallel to the water surface. For the purpose of testing hypothesis #1, the terms (d^2P/dx^2) and (d^2z/dx^2) were calculated from data observed in longitudinal piezometer transects installed in stream beds. The left hand side of equation (5) describes the nature of variations in pressure head in the x direction, whereas the right hand side describes concavities and convexities in

the stream profile. Equation (5) is consistent with the finding by Vaux (1968), that downwelling occurs where the stream profile is convex, and upwelling occurs where the stream profile is concave.

The shape of the water surface profile was surveyed, and the distribution of pressure head in the stream bed was measured from piezometers (Figure 2). This provided the data needed to field-test hypothesis #1. Piezometers could not be driven to exactly the same depths, so a minor correction was made to calculate the pressure distribution along a curve parallel to the water surface profile. Calculating the left-hand-side of equation (5) involved taking the second derivative of the "function" describing pressure distribution in terms of distance in the x-dimension. Calculating the right-hand-side of equation (5) involved taking the second derivative of the "function" describing water surface elevation in terms of distance downstream. I then applied a statistical approach to determine the degree to which the linear relationship defined by equation (5) was satisfied in the piezometer transects.

A numerical technique for differentiation of unequally spaced data (Charpa, 1988) was used to calculate (d^2z/dx^2) and (d^2P/dx^2). The mechanics of this involve calculating the second derivatives of (z) and (P) as functions of (x) for each observation point along piezometer transects. The first derivative at each observation point within the functions was calculated as

$$F'(x) = F(x_{i-1})* (2x - x_i - x_{i+1})/((x_{i-1} - x_i)(x_{i-1} - x_{i+1}))$$
$$+ F(x_i)* (2x - x_{i-1} - x_{i+1})/((x_i - x_{i-1})(x_i - x_{i+1})) \quad (6)$$

$$+ F(x_{i+1})* (2x - x_{i-1} - x_i)/((x_{i+1} - x_{i-1})(x_{i+1} - x_i))$$

where (x) is the value at which the derivative is estimated. Second derivatives were calculated by substituting first derivatives for (x) in equation (6). This method allowed (d^2z/dx^2) and (d^2P/dx^2) to be calculated and compared for each observation point along piezometer transects. The observed and theoretical relationships between (d^2z/dx^2) and (d^2P/dx^2) were then compared.

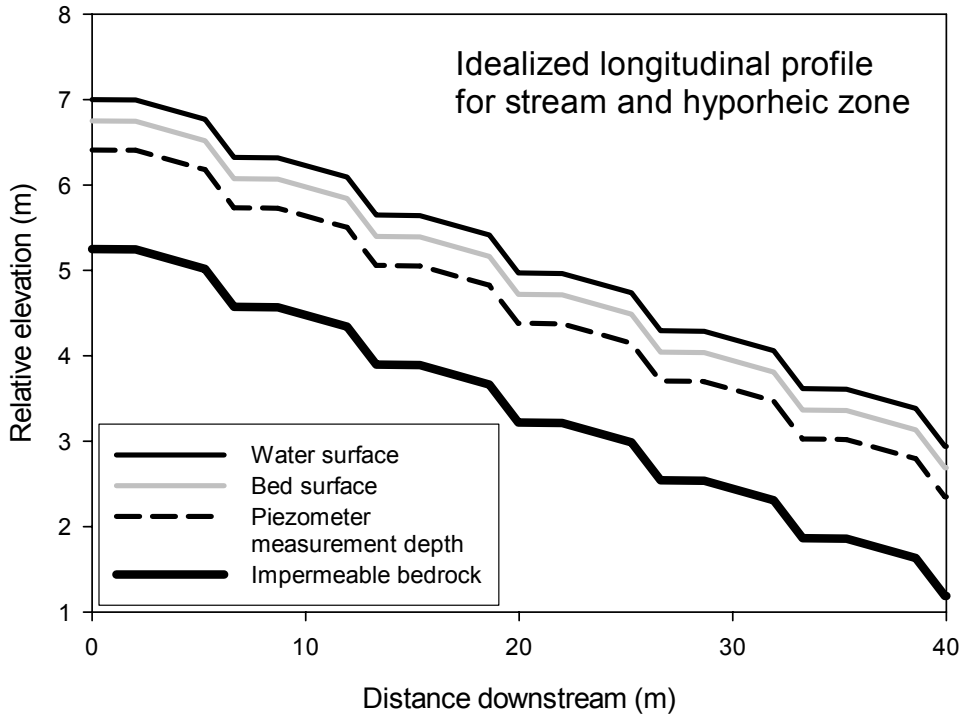

Figure 2: An idealized stream profile for a stream in which the water surface, the bed surface, and the impermeable bedrock are all parallel. Also shown is the targeted depth (34 cm) for pressure head measurements from piezometers used in this study.

2.3.2 Average Water Surface Concavity

I propose an index for quantifying the average water surface concavity (AWSC) for a water surface profile:

$$\text{AWSC} = \left[\sum_{i=1}^{n} \left| d^2 z / dx_i^2 \right| \right] \div n \qquad (7)$$

The index is calculated as the average absolute value of the second derivative for every survey point in the longitudinal water surface profile. AWSC has units of length per unit length squared, and is essentially a roughness metric for the water surface profile.

2.4. STATISTICAL ANALYSIS AND MODELING

2.4.1. Regression models for predicting stream characteristics

Survey and inventory data from randomly selected stream reaches was used to fit regression models for predicting stream reach characteristics. Backwards selection was used to select the most efficient models for predicting each stream characteristic. For explanatory variables, basin area was chosen to represent the location of a stream reach within the river continuum, and stream reach gradient

was chosen because it is easily measured, and has a strong potential for influencing stream characteristics. Each analysis began with a full model that included basin area, stream reach gradient, and an interaction term. Non-significant terms were removed from models. Model selection included a visual inspection of plotted data to ensure a good linear fit. In many cases the data needed to be transformed with the natural logarithm in order to satisfy the assumption of linearity and equal spread implicit in the linear regression analysis.

The first goal in using regression analysis was to identify the most striking patterns in bed configuration across the observed range of basin area and stream reach gradient. The second goal was to predict patterns in stream morphology and quantify the amount of variability explained by predictive models. I did not attempt to make causal inferences from regression models.

I explored patterns in bed configuration by investigating the shape of the water surface profile. Two different approaches for describing the shape of the water surface profile were considered. In one approach, models were developed for predicting the shape of the water surface profile based on observed patterns in CSU spacing and CSU dimensions. In the second approach, models were developed for describing the shape of the water surface profile based on CSU spacing and the relative abundance of CSUs from the different slope categories. The two approaches were compared, and the most powerful models were used in a program for predicting changes in the shape of the water surface profile along the river continuum. Linear regression models were also used to predict stream widths, to

quantify the observed variability in the relationship between the distributions of elevation head and pressure head described by equation (5), and for predicting the length of downwelling zones from basin area.

The models for predicting the relative abundance of CSUs satisfy the assumption of independence inherent in the regression analysis. These are summary statistics for stream reaches that are spatially separated by long distances. The possibility of serial correlation in the models for predicting CSU spacing, stream width, and stream depths can not be ruled out, so the results must be interpreted cautiously. Any serial correlation present is expected to affect the standard errors and the confidence intervals for the regression coefficients, but it is not expected to cause a bias in the least squares estimate of the regression coefficients, (Ramsey and Schafer, 1997). The statistical models were verified by comparing model output to observed data for a stream reach that was not used to parameterize models. These results provide support that serial correlations have not confounded the results.

2.4.2 Program design – idealized stream reach longitudinal profiles

Longitudinal profiles of idealized stream reaches were created based on output from regression models developed for predicting average stream characteristics from data measured in the randomly selected stream reaches. A

single program that incorporates the entire set of regression models creates idealized longitudinal profiles for any specified value of drainage basin area and average stream reach gradient observed within the study area. Throughout this study I focus on how the shape of the water surface profile influences upwelling and downwelling in different stream reaches. Idealized profiles summarize predictions of stream feature frequency, size, spacing, and gradient into a comprehensive prediction for the shape of the water surface profile.

3. RESULTS

3.1. STREAM GEOMORPHOLOGY

3.1.1. Lateral complexity in stream reaches

3.1.1.1. Widths

Regression models were used to quantify changes in the wetted stream channel width, active channel width, and the confined channel width across the range of basin area observed in the randomly selected stream reaches (Table 4). Basin area explained between 57% and 70% of the observed variability in widths.

After accounting for basin area, the affect of stream reach gradient was insignificant for predicting active and confined widths. Stream reach gradient was significant, but only slightly improved the model for predicting wetted width after accounting for basin area.

Table 4: Regression models for predicting stream widths

Parameter	**model**	**n**	**R^2**	**2-sided p value**
Median wetted width	= Exp(1.05 + 0.33(ln(AREA)))	156	.567	<0.0001
Median active width	= Exp(1.40 + 0.31(ln(AREA)))	156	.697	<0.0001
Median confined width	= Exp(1.71 + 0.32(ln(AREA)))	156	.684	<0.0001

3.1.1.2. Frequency of bars and secondary channels

All but one of the randomly selected stream reaches had some secondary channel development. Most of the secondary channels observed were channel splits separated from the main channel by island bars or transverse bars (Table 5). In second-order streams bars tended to be small, poorly developed, poorly sorted and associated with large, essentially immobile boulders or wood. In third-order

streams bars were larger, better developed, and had sediment that was better sorted. Bars in fourth-order streams were the largest, most well developed, and sediment was the most well sorted. One channel split, observed in an unconfined reach (416.1), was not connected to the main channel at the downstream end. An alcove was observed in the bedrock reach (403). The alcove was associated with a scoured depression between a gravel/cobble bar, and a bedrock wall confining the active floodplain.

Table 5: Summary of stream reach confined widths, secondary channels, and bars

Reach	Area	Relative % of average confined width	% of total length in secondary channels	Secondary channel number	Secondary Channel type	Secondary channel length	Exposed bar area
282	0.62	132.71	10.96	1	channel split	3.7	2.68
				2	channel split	3.0	1.95
				3	channel split	3.85	3.85
241	1.04	101.17	11.98	1	channel split	6.6	4.67
214	1.12	58.31	10.48	1	channel split	6.5	6.88
395	1.34	115.48	28.02	1	channel split	8	9.6
				2	channel split	21.35	48.5
224	1.98	85.04	7.98	1	channel split	7.2	8.76
348	3.85	114.71	11.42	1	channel split	16.7	21.72
333	5.21	111.94	35.02	1	channel split	46.1	136.28
356	16.87	114.25	14.04	1	channel split	28.4	62.02
416	53.86	105.23	100	1	Distinct side channel	256	NA
416.1	53.86	105.23	25.64	1	channel split	38	116.22
				2	channel split	17.25	17.68
				3	channel split	47.45	340.21
416.2	53.86	105.23	37.42	1	channel split	54.1	211.58
				2	channel split	20.3	8.87
				3	channel split	23	46.15
403	62.35	78.33	8.77	1	Alcove	23.45	49.39

Bar-formed secondary channel lengths and the dimensions of island bars certainly increase with increasing drainage basin area (2-sided p-values <0.001 from simple linear regression). However, I found no evidence to suggest that the length of bar-formed secondary channels, relative to surveyed reach lengths, increased with increasing basin area (2-sided p-value = 0.95 from simple linear regression). The mean length of bar-formed secondary channels as a proportion of surveyed reach length was 21.0%.

There was a significant relationship between the channel confinement and the length of bar-formed secondary channels, relative to the stream reach length. Grouping streams with above average confined widths for a given basin area, and those with below average confined widths allows for a statistical comparison of mean secondary channel length for the two groups. The estimated mean secondary channel length as a percentage of total reach length are 9.1% in relatively confined stream reaches, and 23.4% in relatively unconfined stream reaches (2-sided p-value = .039 from a 2-sample t-test). However, a regression of relative side channel length on relative confinement was not significant.

Distinct side channels associated with islands above the active flood plain occurred in only one of the randomly selected stream reaches (Table 5). The confined width for this stream reach was above average. Though islands are expected to be more common in unconfined stream reaches, this relationship could not be tested with the available data.

3.1.1.3. Cross-valley hydraulic gradients

Stream reach survey data were used to make comparisons between cross-valley hydraulic gradients and longitudinal hydraulic gradients. Where channel splits and alcoves were present, the steepest cross-valley gradients always exceeded the average longitudinal gradient. Average cross-valley gradients exceeded average longitudinal gradients in 7 out of 13 stream reaches (Table 6). Cross-valley gradients were not measured in two fourth-order stream reaches where secondary channels were not present. Regression models predicted that average cross-valley gradients would be nearly equal to, or slightly greater than average longitudinal gradients (equations 22 and 23 in Table 7) in stream reaches throughout the observed range of basin area. As basin area increases, longitudinal gradients are predicted to decrease slightly more rapidly than cross-valley gradients (Figure 3). Considering also the marked increase in bar area with increasing basin area, the end result is that the potential for cross-valley gradients to alter the direction of hyporheic flowpaths increases with basin area.

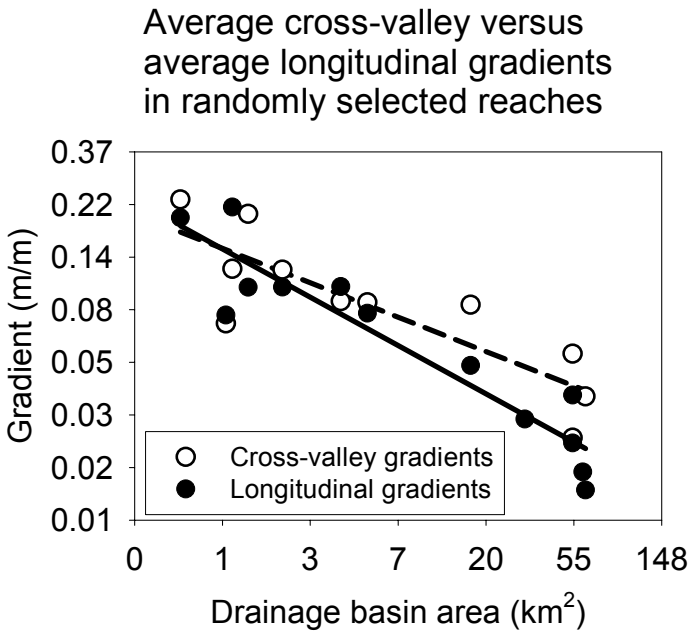

Figure 3: Predicted cross-valley and longitudinal gradients. The solid line indicates predicted longitudinal gradients and the dashed line indicates predicted cross-valley gradients.

Table 6: Summary of cross-valley gradients in stream reaches

Reach	Area (km^2)	Avg. reach gradient (m/m)	Avg. cross-valley gradient (m/m)	Steepest cross-valley gradient (m/m)
282	0.62	0.202	0.234	0.447
241	1.04	0.078	0.072	0.325
214	1.12	0.218	0.121	0.240
395	1.34	0.102	0.204	0.761
224	1.98	0.102	0.12	0.260
348	3.85	0.102	0.089	1.270
333	5.21	0.079	0.088	0.732
356	16.87	0.048	0.086	0.741
428	31.29	0.027	0	0
416.1	53.86	0.023	0.054	0.135
416.2	53.86	0.036	0.024	0.825
407	60.46	0.018	0	0
403	62.35	0.015	0.036	0.046

3.1.2. Longitudinal patterns in stream reaches

3.1.2.1. CSU spacing, size, and relative abundance

Watershed area was the variable chosen to represent the position of a stream reach within the river continuum. Regression models for predicting stream characteristics from basin area and stream reach gradient had varying degrees of success (Table 7). Changes in bed configuration along the river continuum are represented by changes in CSU spacing, size, and the relative abundance of CSUs with increasing basin area (Table 8). The differences in how the effects of basin area are interpreted result from differences in data transformations in the regression models. In some cases the natural logarithm transformation was performed on the explanatory variable, sometimes on the response variable, and sometimes on both. Regression models showed that increases in drainage basin area were associated with a significant increase in the percent of total reach length contained in FLATs, and significant decreases in the percentages of total reach length contained in STEEPs and STEPs. The absolute length of FLATs and STEEPs increased significantly, however, no significant increase in STEP length was detected. Increases in basin area were also associated with a significant decrease in the percent of total reach height contained in STEPs, and a significant increase in the percent of total reach height contained in STEEPs. The distance between STEPs, and the distance between FLATs both increased significantly with basin area.

Table 7: Regression models for predicting stream reach characteristics. Equations 10 – 21 were used to parameterize idealized longitudinal profiles.

Parameter	Model	n	R^2	2-sided p-value	Eq. numb
Median STEP.dist	= Exp(2.53 + 0.29(ln(AREA)) - 6.57(GRAD) - 2.46(ln(AREA*GRAD)))	112	.498	<0.0001	10
Mean %FLAT.Length	= 44.81 + 10.16(ln(AREA) - 129.81(GRAD) - 112.17(ln(AREA)*GRAD)	13	.942	<0.0001	11
Median %STEP.length	= Exp (1.99 - 0.047(AREA) + 9.07(GRAD) + 0.96(AREA*GRAD))	13	.944	<0.0001	12
%STEEP.length	= 100 - %FLAT.length - %STEP.length	na	na	na	13
Median %FLAT.height	= Exp (0.71 + 0.04(AREA) – 9.32(GRADIENT))	12	.813	0.0005	14
Mean %STEP.height	= 34.30 – 6.96(ln(AREA)) + 277.40(GRADIENT) + 113.52(ln(AREA)*GRADIENT)	13	.887	0.0001	15
%STEEP.height	= 100 - %FLAT.height - %STEP.height	na	na	na	16
Median FLAT.depth.max	= Exp (2.83 + 0.40(ln(FLAT.length)))	183	.283	<0.0001	17
Median FLAT.depth.min	= Exp(2.39 + 0.18(ln(AREA)))	183	.157	<0.0001	18
Median %FLAT.ht	= Exp(-0.72 + 0.85(lnAREA))	10	.775	<0.001	19
Median %STEP.ht	= 76.56 – 12.92(lnAREA)	11	.75	<0.001	20
Median %STEEP.ht	= 24.80 + 8.43(lnAREA)	11	.53	<0.01	21
Median longitudinal gradient	= Exp (-1.92 - 0.46(ln(AREA)))	11	.88	<0.0001	22
Median Cross-valley gradient	= Exp (-1.92 - 0.33(ln(AREA)))	9	.72	<0.001	23

Stream reach gradient and the interaction between area and gradient significantly improved several model fits, reflecting that gradient affects stream characteristics differently at different basin areas (Table 7). This is reasonable given that stream reach gradient reflects local geology, stream sediment transport

capacity, and the legacy of past flood events and debris inputs, all of which are likely to vary with basin area. Significant models were also fit for predicting increases in the water depth in FLATs with increasing FLAT length and basin area (Table 7).

Table 8: Summary of changes in bed configuration with increasing drainage basin area

Geomorphic variable	Change with increasing drainage basin area	95% confidence bounds for estimated effect
% total reach length in FLATs	Increases by 8.01% for every doubling in basin area	5.81% to 10.22%
% total reach length in STEEPs	Decreases by 0.3% for every increase in area of 1 km^2	0.09% to 0.51%
% total reach length in STEPs	Decreases by 4.6% for every increase in area of 1 km^2	3.2% to 5.9%
FLAT length	Increases by 2.3% for every increase in basin area of 1 km^2	1.8% to 2.8%
STEEP length	Increases by 0.65% for every increase in basin area of 1 km^2	0.60% to 0.70%
% total reach height in STEEPs	Increases by 5.84% for every doubling of basin area	2.38% to 8.43%
% total reach height in STEPs	Decreases by 8.96% for every doubling in basin area	5.48% to 12.44%
Distance between STEPs	Increases by 36% for every doubling in basin area	28% to a 45%
Distance between FLATs	increases by 1.25% for every increase in basin area of 1 km^2	0.80% to 1.68%

Table 9: Frequency and relative importance of STEPs by stream reach and by cause

Reach	Basin area	Avg. reach gradient	Reach length	# of wood-caused STEPs	% reach height casued by wood STEPs	# of rock-caused STEPs	% reach height caused by rock STEPs	Reach length divided by # of STEPs
282	0.62	0.202	62	1	2.1	18	84.7	5.64
241	1.04	0.078	96.25	0	0	6	47.3	5.07
214	1.12	0.218	55.1	3	15.9	8	73.5	9.18
395	1.34	0.102	104.74	3	37.8	7	39.1	10.47
224	1.98	0.102	90.2	4	19.2	10	48.7	6.44
348	3.85	0.102	146.2	2	10	17	56.8	8.12
333	5.21	0.079	131.65	2	21	9	32.5	11.97
356	16.87	0.048	202.28	0	0	14	52.9	14.45
428	31.29	0.027	199.55	0	0	5	27.1	39.91
416.1	53.86	0.023	400.6	0	0	8	23.2	50.08
416.2	53.86	0.036	260	0	0	7	43	37.14
407	60.46	0.018	278.4	0	0	4	29.9	69.60
403	62.35	0.015	267.5	0	0	1	7	267.50

3.1.2.2. Frequency and cause of steps

Wood caused STEPs occurred in all but one second order reach, and in all but one third order reach, but did not occur in any of the fourth order reaches (Table 9, Figure 4). In all cases, rock-caused STEPs were more common than wood-caused STEPs. These included cobble-, boulder-, and bedrock-caused STEPs. Consequently the percent of stream reach height (elevation drop) comprised by rock steps was higher than the percent of stream reach height comprised by wood steps (Figure 4). However, on average wood-caused STEPs

were both steeper (2-sided p-value = 0.002 from a 2-sample t-test) and taller (2-sided p-value = 0.013 from a 2-sample t-test) than rock-caused STEPs (Figures 5 and 6). The average slope for wood-caused STEPs was 47.3% compared to 28.6% for rock-caused STEPs. The average height for wood caused STEPs was 0.69 meters compared to 0.45 meters for rock-caused STEPs.

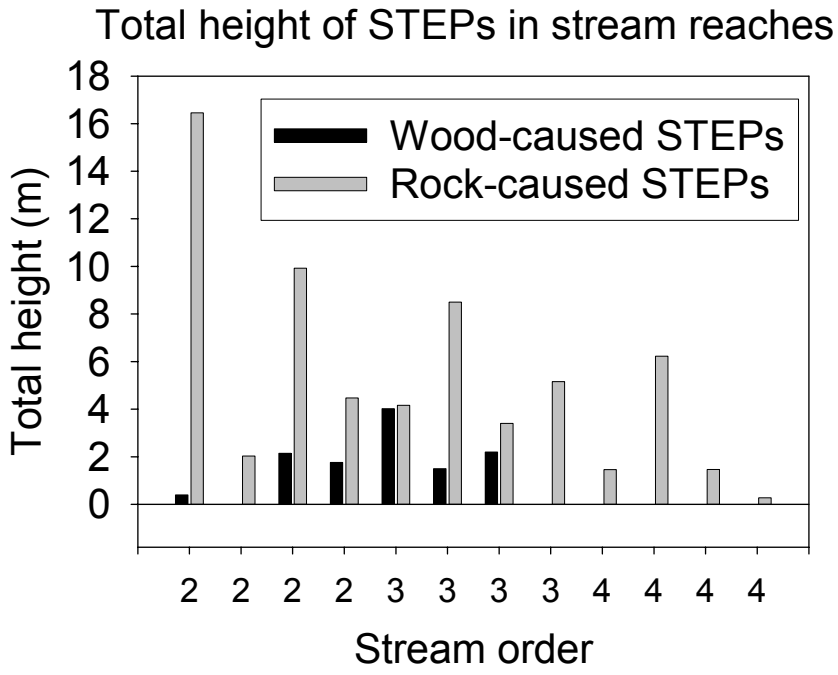

Figure 4: Total height of STEPs by cause within second-, third-, and fourth-order survey reaches.

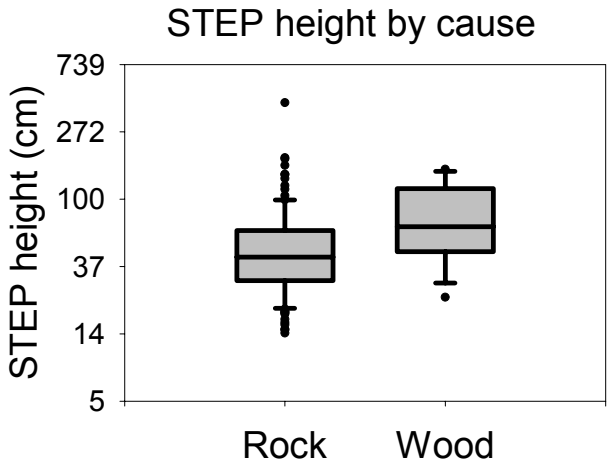

Figure 5: Comparison of STEP height by cause

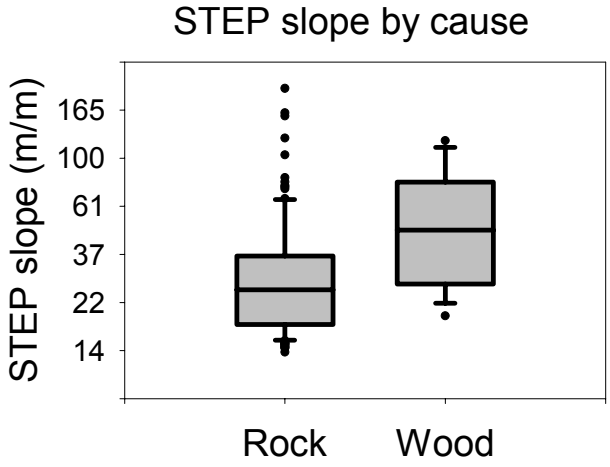

Figure 6: Comparison of STEP slope by cause

3.1.2.3. Idealized Longitudinal profiles

Regression models were incorporated into a single program for predicting the general shape of water surface profiles for any given point in the river continuum, within the range of basin areas surveyed. The most powerful approach for predicting the shape of water surface profiles was to use the predicted median distance between STEPs to set the spacing for a repeating pattern of slope breaks, and the predicted relative abundance of CSUs to determine the dimensions for slope breaks between STEP locations. STEP locations and dimensions were determined first, and then the spaces between steps was allocated to FLATs and STEEPs according to the predicted relative distance and height proportions. This approach was chosen because the models for predicting the spacing between STEPs and the relative abundance of CSUs explained much more variability than did the models for predicting CSU lengths. The selected set of regression equations comprises a single program for predicting the average shape of the water surface profile for any value of basin area and average stream reach gradient observed in the Lookout Creek Basin. Idealized longitudinal profiles are homogeneous in the pattern, size, and spacing of CSUs, and are programmed to represent one of two commonly observed patterns; FLAT, STEEP, STEP (for headwater streams); or FLAT, STEP, STEEP (for mid-order streams) (Figure 7). Observed profiles were more complex, but the idealized profiles appear to capture the observed patterns in average bed form spacing.

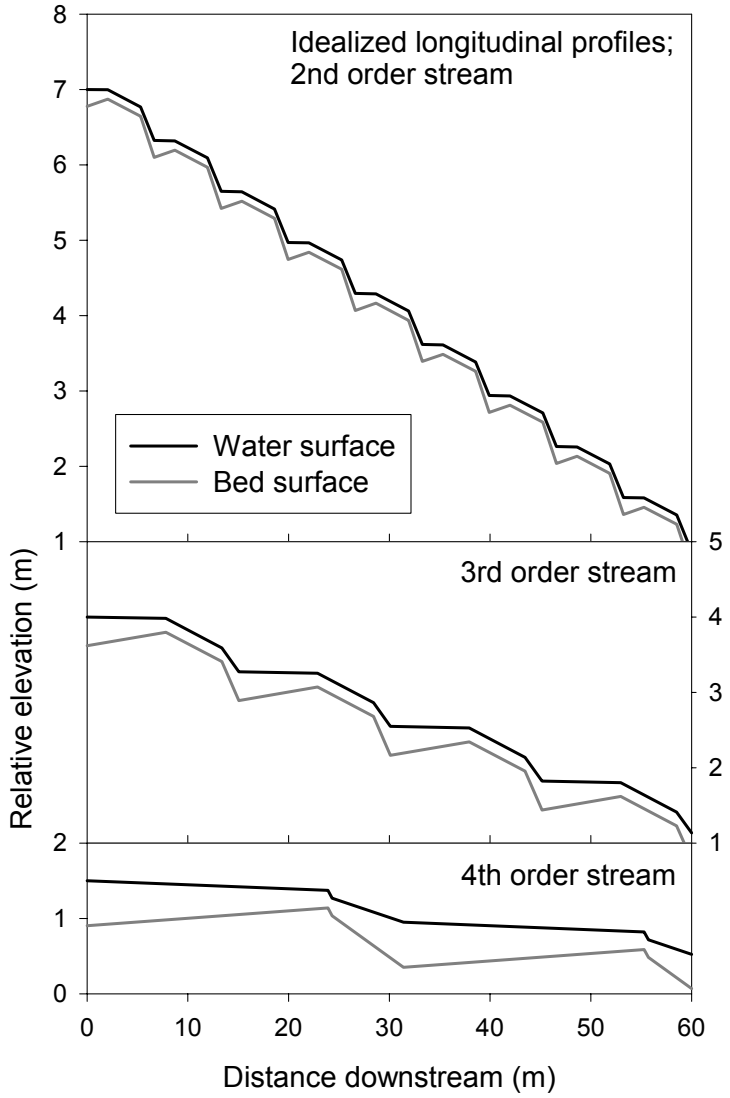

Figure 7: Examples of idealized longitudinal profiles for 2nd order, 3rd order, and 4th order streams. These idealized profiles were predicted for stream reaches having drainage basin area equal to 2.0 km^2 (2nd order), 16.9 km^2 (3rd order), and 60.5 km^2 (4th order), with average reach gradients of 10.2%, 4.8%, and 1.8%, respectively. The 2nd, and 3rd order profiles have the pattern FLAT, STEEP, STEP, whereas the 4th order profile has the pattern FLAT, STEP, STEEP.

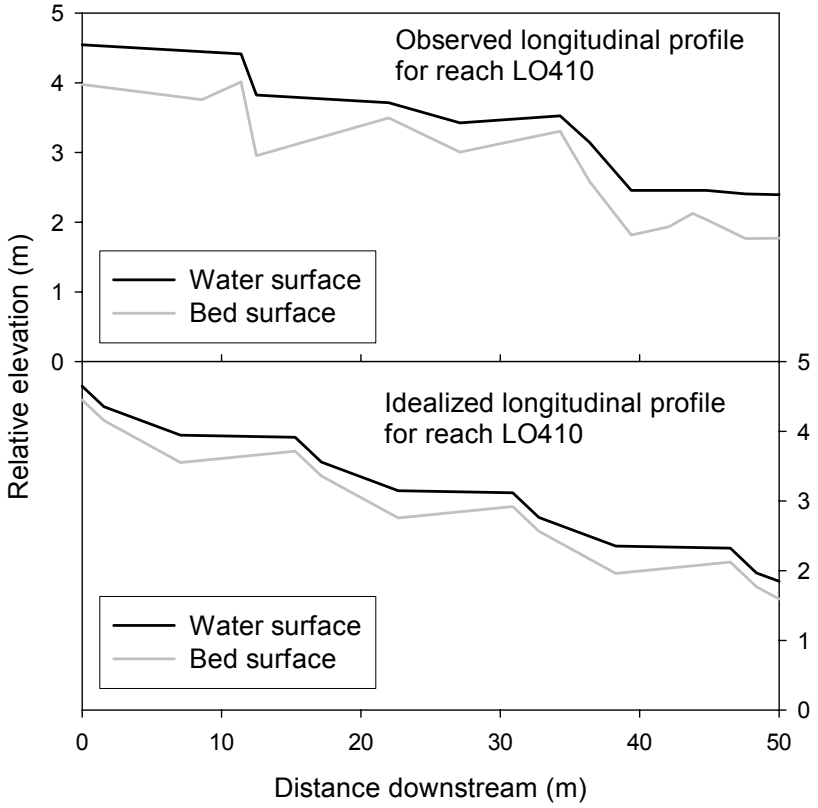

Figure 8: Comparison of idealized and observed longitudinal profiles for LO 410

Table 10: Predicted and observed stream characteristics for LO410, a stream reach that was not used to parameterize regression models. Lower and upper bounds of 95% confidence intervals for estimates are included for comparison.

Characteristic	Predicted value	Observed value	Lower 95%CI	Upper 95%CI
Mean STEP.dist	16.19	15.86	11.54	21.10
Mean FLAT.LENGTH	8.21	9.98	7.05	9.37
Mean STEEP.LENGTH	5.50	4.44	2.96	7.44
Mean STEP.LENGTH	1.88	1.68	1.09	3.28
Mean FLAT.HEIGHT	0.03	0.06	0.02	0.06
Mean STEEP.HEIGHT	0.41	0.48	0.29	0.52
Mean STEP.HEIGHT	0.35	0.51	0.26	0.45
Mean WET.WIDTH	8.59	9.06	7.87	9.38
Mean MAX.DEPTH	0.39	0.66	.35	.44
Mean MIN.DEPTH	0.20	0.42	.18	.22

3.1.2.4. Idealized profile verification

The program for producing idealized longitudinal profiles was verified by comparing output to observed data. Stream reach LO410, a reach that was not used to parameterize the set of regression models used in the program, was used for comparison. LO410 is a fourth-order, 259 meter-long reach located on main stem Lookout Creek that has a basin area of 25.9 square kilometers and an average gradient of 4.84% (Figure 1). The program generally performed well. The idealized profile looks much like the observed profile (Figure 5), and the majority of observed mean values fell within the 95% confidence interval for the predicted

means (Table 10). However, the program under predicted the mean FLAT length, STEP height, and the depth of FLATs. This may be due to the presence of a few uncharacteristically large pools, and a small waterfall in LO 410. Despite these, the program produced satisfactory results.

3.1.2.5. Water surface concavity

AWSC (Eq. 7) generally decreased with increasing basin area (Figure 9). It is estimated that AWSC decreases by 0.013 m/m^2 for every doubling in drainage basin area within the observed range of data (p-value < 0.0001 from simple linear regression; $R^2 = .87$). AWSC was highest where step-pool development was most pronounced or where water surface profiles were highly irregular (Figure 10).

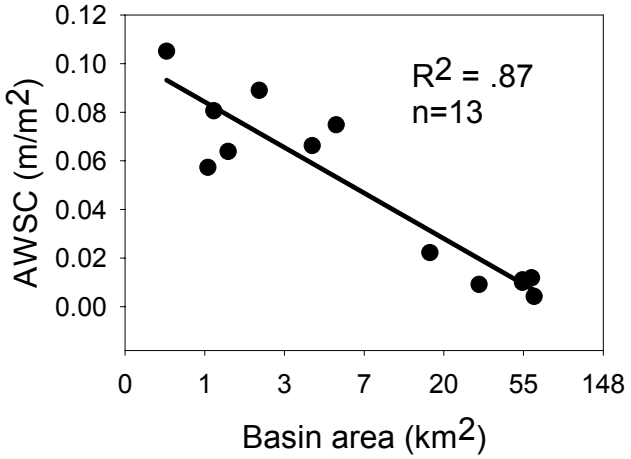

Figure 9: Observed and predicted relationships between AWSC and drainage basin area

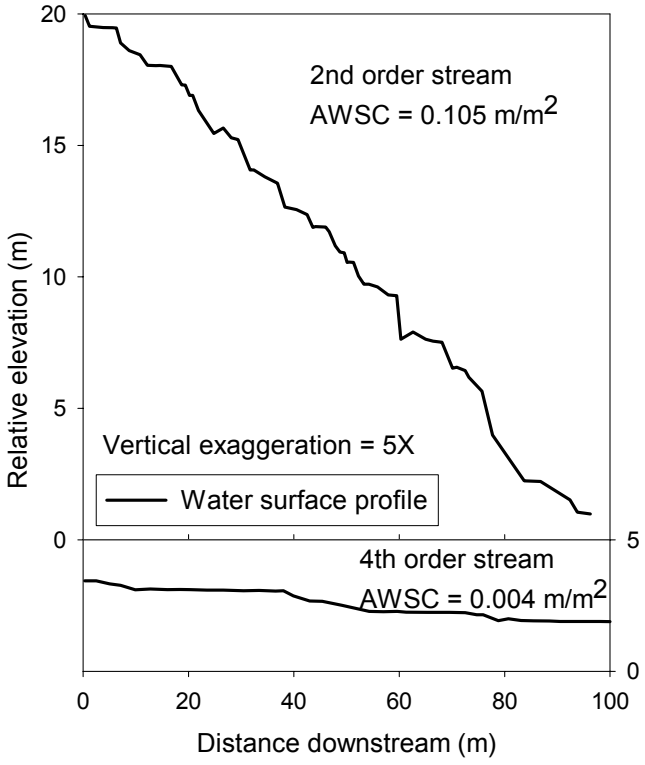

Figure 10: Examples of water surface profiles with varying values of AWSC

3.2. PIEZOMETER TRANSECTS

3.2.1 Hypothesis #1

Water surface profiles and pressure head data from piezometer transects were analyzed to calculate (d^2z/dx^2) and (d^2P/dx^2) (Eq. 6), and compared to the

relationship expected from equation (5) (Figures 11 and 12). The amount of variability explained by the observed relationships provides a measure of the degree to which the assumptions of the theoretical model are justified.

For all piezometer transects combined, statistical analysis shows that approximately 38% of the variability in the pressure head distribution measured in stream beds was explained by the elevation head distribution along the water surface profile (Figure 8). The least squares regression model fit is

$$(d^2P/dx^2) = -1.2558(d^2z/dx^2) - 0.0123 \qquad (8)$$

and is similar to equation (5). The estimated slope is nearly 26% steeper than expected, but the 95% confidence interval for the estimate (-0.84 to –1.66) contains the ideal slope.

Model performance in individual piezometer transects varied (Table 11). The slope describing the relationship between (d^2z/dx^2) and (d^2P/dx^2) varied between -0.78 and –2.06 (figures 13, 14 and 15). The amount of variability described by the theoretical relationship varied between 14% and 67% (Table 11). The best results came from piezometer transect P224.1 in the well developed step-pool channel. The poorest results comes from P224.0, where the pool-step morphology is poorly defined. A comparison of data from all three piezometer transects shows that the magnitude of values of (d^2P/dx^2) increased with increasing AWSC (Table 11, Figure 16). The null hypothesis associated with hypothesis #1 states that the distribution of pressure head within the hyporheic zones of real

streams is independent of the shape of the water surface profile. The results presented here provide sufficient evidence to reject the null hypothesis.

Table 11: Results from regression models for quantifying the observed relationship between (d^2P/dx^2) and (d^2z/dx^2) in piezometer transects. AWSC values are included for comparison.

Piezometer transect	n	slope	R^2	p-value	AWSC (m/m^2)
P224	18	-1.79	.14	0.12	0.037
P224.1	14	-1.24	.67	<0.001	0.122
P356	30	-0.78	.18	0.02	0.021
All transects	62	-1.26	.38	<0.0001	na

A limitation of the analytical technique used to test hypothesis #1 is that there were many potential sources of error. Difficulty in driving piezometers to equal depths and equal spacing intervals required data corrections and numerical differentiation of unequally spaced data. Numerical derivation amplifies error in original data (Charpa, 1988). The testing of hypothesis #1 required comparing data after numerical differentiation of separate functions, allowing potential errors to be amplified again.

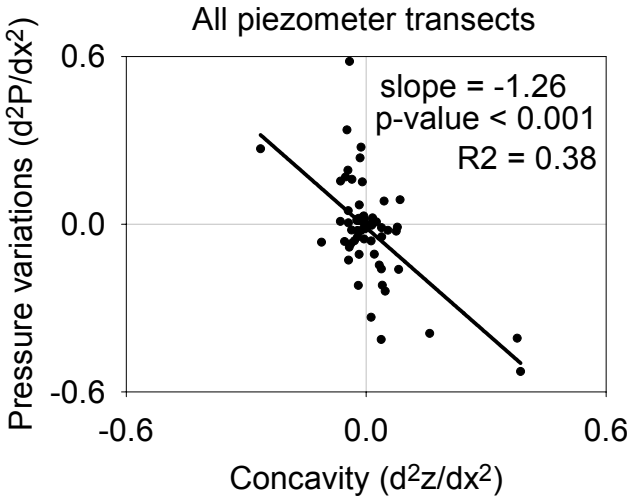

Figure 11: Observed relationship between the distribution of elevation head along the water surface profile of a stream, and the distribution of pressure head in the stream bed: all piezometer transects

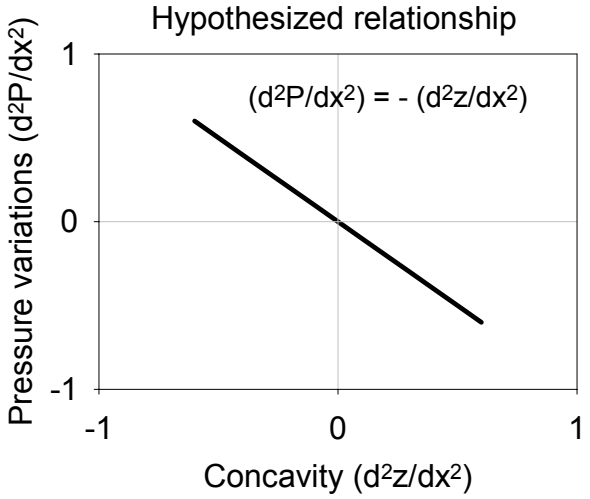

Figure 12: Ideal relationship between the elevation head distribution along the water surface profile of a stream, and the pressure head distribution in the bed of the stream, as predicted by the theoretical model

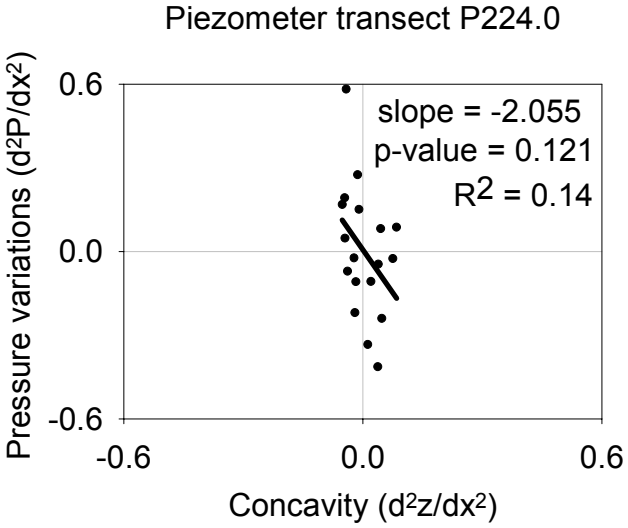

Figure 13: Observed relationship between the distribution of elevation head along the water surface profile of a stream, and the distribution of pressure head in the stream bed: piezometer transect P224.0

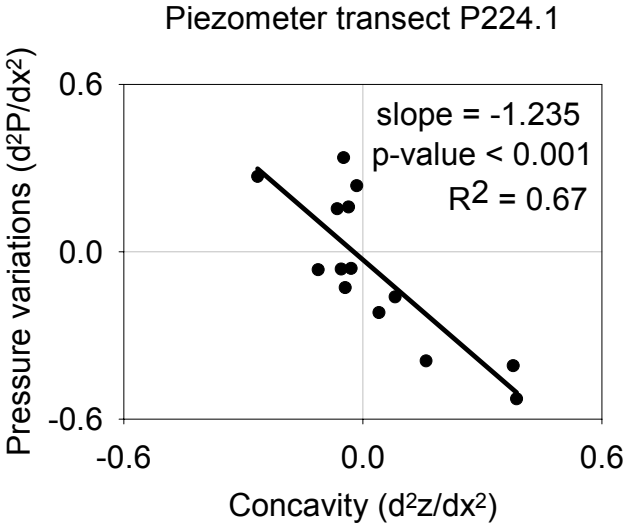

Figure 14: Observed relationship between the distribution of elevation head along the water surface profile of a stream, and the distribution of pressure head in the stream bed: piezometer transect P224.1

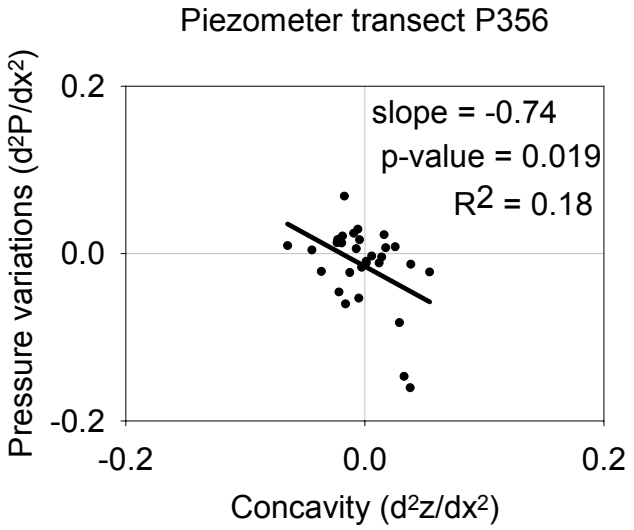

Figure 15: Observed relationship between the distribution of elevation head along the water surface profile of a stream, and the distribution of pressure head in the stream bed: piezometer transect P356. Note that the scale is small on this graph, and that the range of observed values is narrow compared to other piezometer transects.

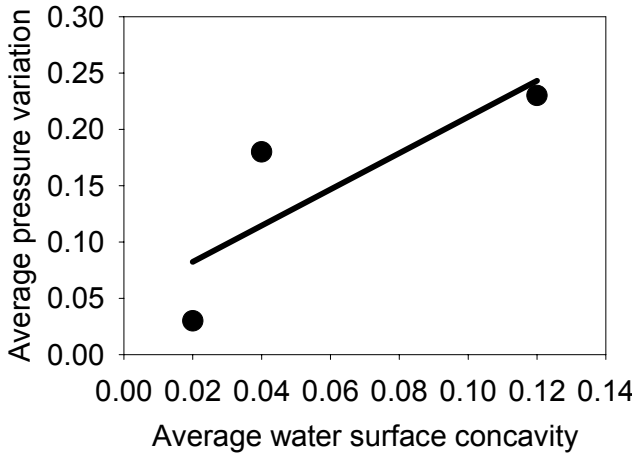

Figure 16: Relationship between the average absolute value of pressure variations and the average absolute value of concavity in the three piezometer transects

Concavity correctly predicted upwelling or downwelling locations 83% of the time in P224.0 (Figure 17), 71% of the time in P224.1 (Figure 18), and 63% of the time in P356.0 (Figure 19). Overall predictions were correct in 71% of the cases.

A regression model was fit for predicting changes in VHG from changes in elevation along the water surface profile:

$$\text{Mean}(\Delta VHG) = 0.1901 - 2.4754(\Delta ELEV) \quad (9)$$

Results show an inverse relationship between changes in VHG and changes in water surface elevation. This model predicts that VHG in the stream bed will increase, on average, by 2.48 meter/meter for every 1 meter/meter drop in water surface elevation (95% CI from 1.35 m/m to 3.60 m/m).

Equations (8) and (9) use only changes in water surface elevation to explain approximately 38% and 22%, respectively, of the observed variation in pressure head distributions and VHG along the piezometer transects. The variability not explained by the shape of the water surface profile is likely due to the effects of a combination of underlying bedrock topography, the presence of large buried boulders, discontinuities in hydraulic conductivity, cross-valley hydraulic gradients and convection-driven pressure gradients.

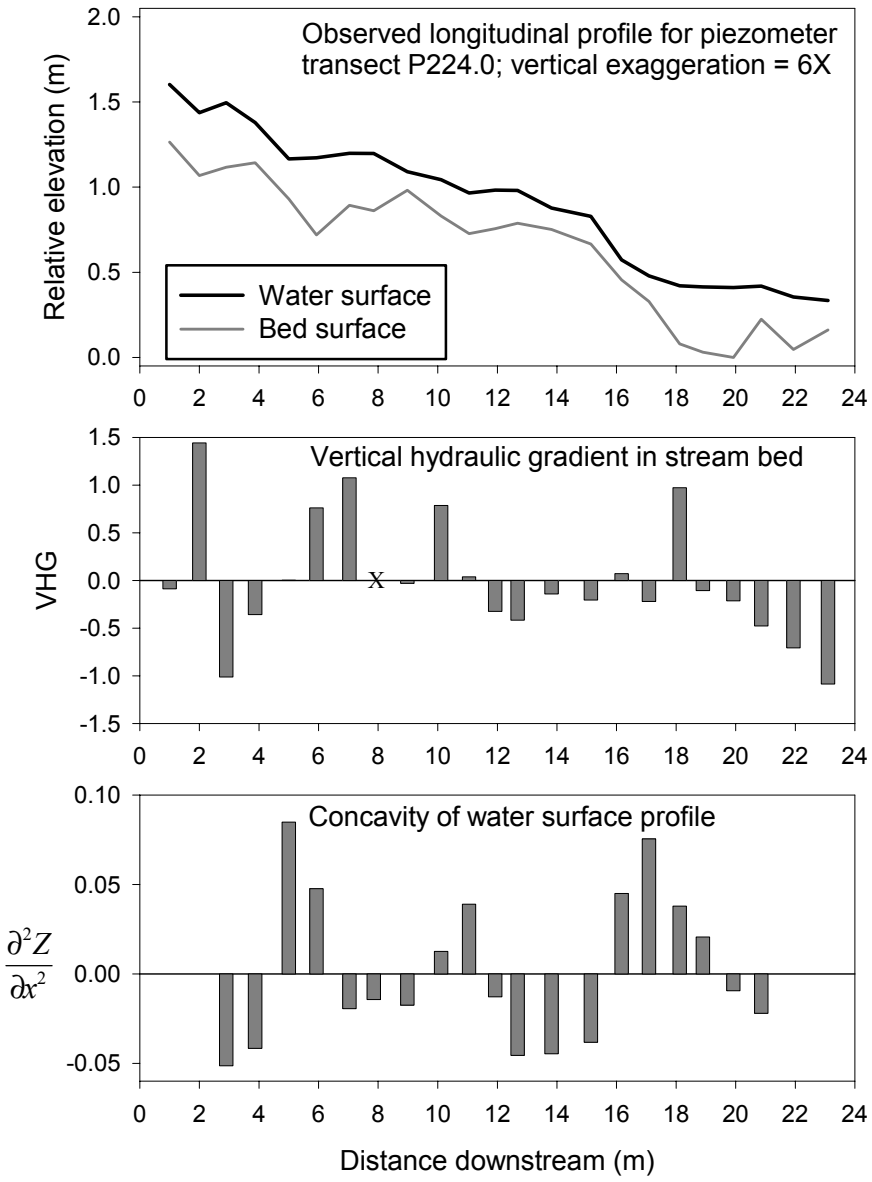

Figure 17: Observed longitudinal profile, vertical hydraulic gradients, and water surface concavity for piezometer transect P224.0. "X" indicates missing data.

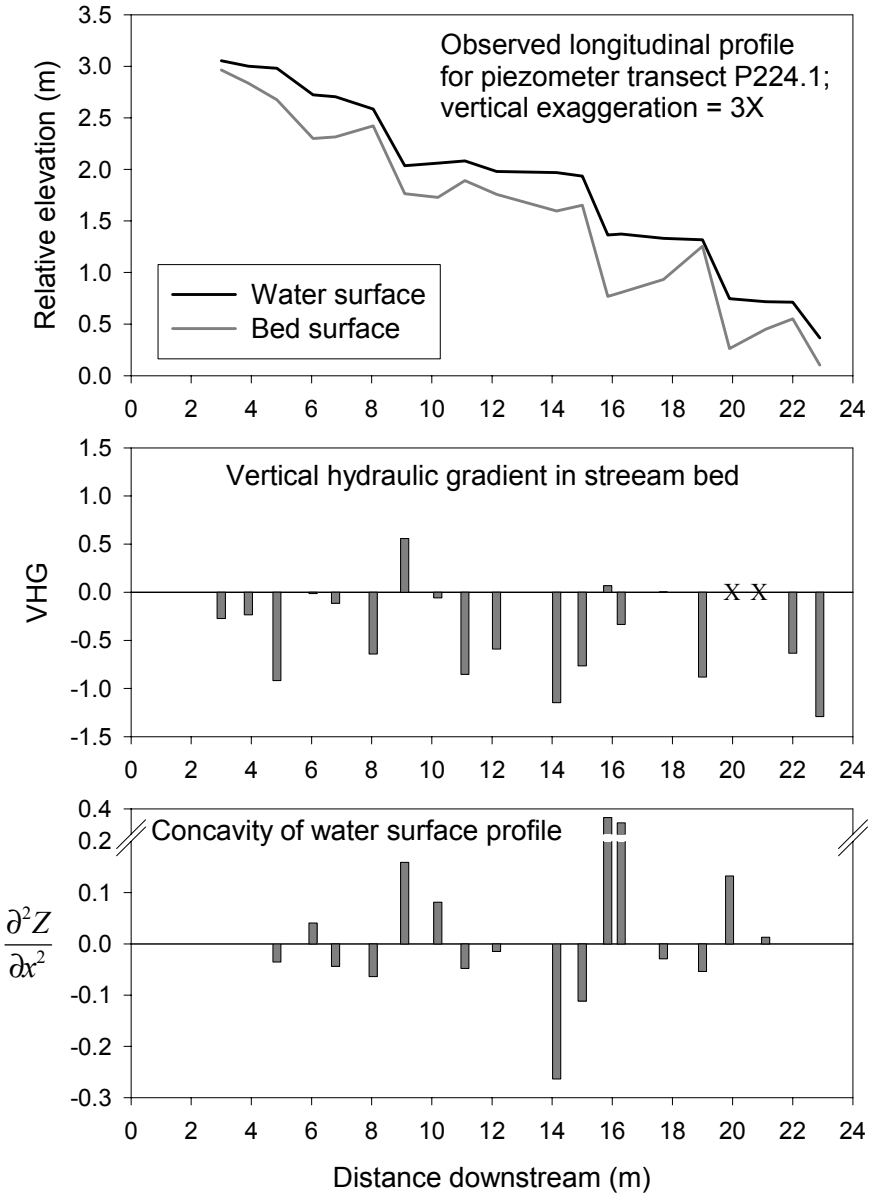

Figure 18: Observed longitudinal profile, vertical hydraulic gradients, and water surface concavity for piezometer transect P224.1. "X" indicates missing data.

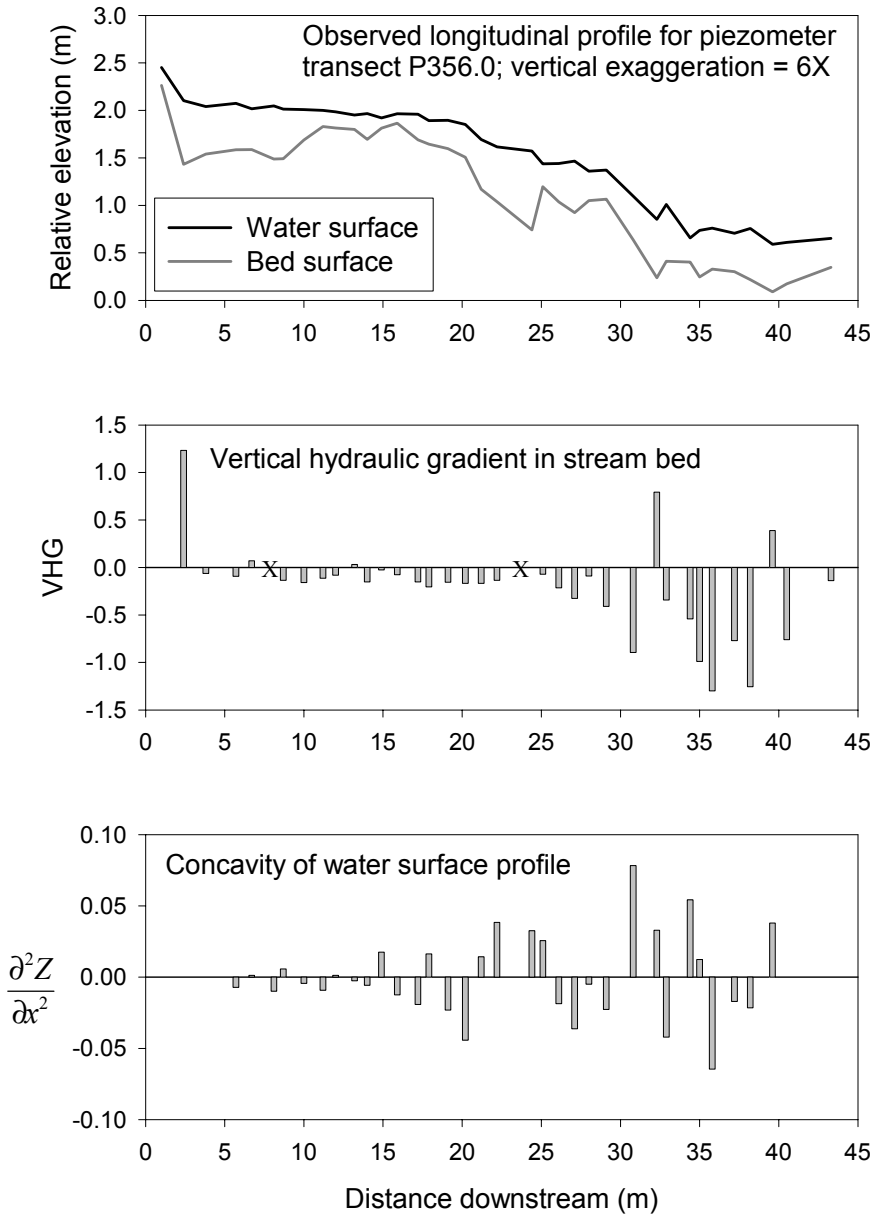

Figure 19: Observed longitudinal profile, vertical hydraulic gradients, and water surface concavity for piezometer transect P356.0. "X" indicates missing data.

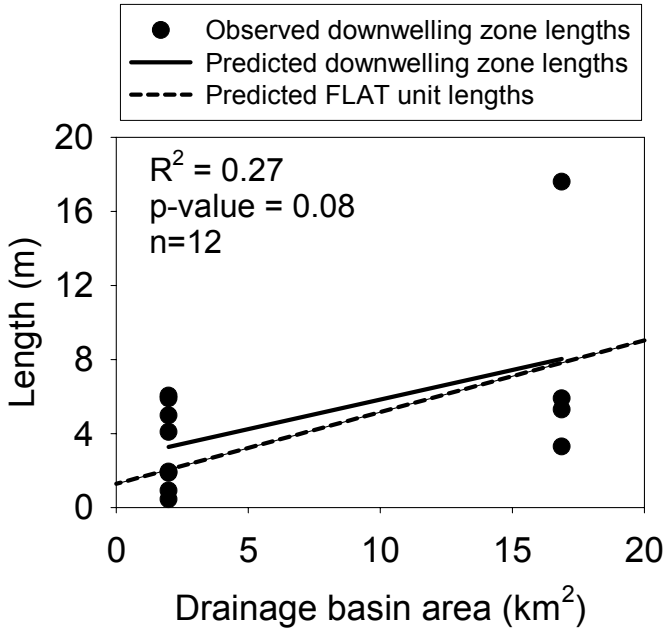

Figure 20: Relationship between basin area and downwelling zone length. Note that average the average length of FLAT units predicted for idealized profiles nearly matches the average downwelling zone length over the observed range in basin area.

3.2.2 Hypothesis #2

Six downwelling zones were identified in P224.0, three were identified in P224.1, and five were identified in P356. Two downwelling zones were omitted from the data set because they occurred in only 1 or 2 piezometers at an end of a piezometer transect, and the entire length of the downwelling zone may not have been captured. The length of downwelling zones increased with increasing basin

area (2-sided p-value = 0.082). The null hypothesis, that the reach average downwelling zone length is independent of basin area and the position of a stream reach within the river continuum, is rejected. It is estimated that downwelling zone length increases by approximately 32 cm for every increase in basin area of 1 km^2. A 90% confidence interval for the increase is from 2 cm to 62 cm. This increase nearly matches the increase in length predicted for FLATs in the idealized longitudinal profiles (Figure 20).

4. DISCUSSION

4.1. STREAM GEOMORPHOLOGY AND HYPORHEIC EXCHANGE FLOW

4.1.1. Lateral complexity in stream reaches

Channel confinement affected the relative abundance of bar-formed secondary channels in stream reaches, however, the position of a stream reach within the river continuum did not (table 5). With increasing basin area, bar size and secondary channel length increased, but the only other observed patterns concerning secondary channel and bar development observed were qualitative. The degree of bar development and sediment sorting increased with increasing basin

area, and certain secondary channel types occurred only in mid-order reaches. Where secondary channels did occur, cross-valley hydraulic gradients tended to be steeper than longitudinal gradients. Steep cross-valley gradients increase cross-valley hyporheic exchange flow, which has the effect of increasing hyporheic residence times (Kasahara and Wondzell, in press). An increase in bar area and a slight increase in the relative importance of cross-valley gradients compared to longitudinal gradients suggested that the potential for cross-valley hyporheic exchange flow increases with distance downstream.

The objectives of this study included examining stream reach geomorphology for patterns that are expressed over a portion of the river continuum, and that are predictable from easily measured drainage basin characteristics. For the sake of efficiency, stream reaches were chosen according to a random sampling design, stratified by stream order. The scale of this study may have been too small to capture strong trends in the lateral complexity of stream reaches along the river continuum. Additionally, confinement is a relative measure, and this study area did not capture a large sample of reaches with a wide range of confinement at different basin areas. The results of this study suggest that channel confinement may be a useful metric in the search for patterns in stream geomorphology that affect hyporheic exchange flow, however, selecting stream reaches according to channel confinement would likely require a larger study area and a different sampling design.

4.1.2. Relative Importance of steps and riffles

Patterns in the relative proportions of CSUs have implications for ranking the importance of different kinds of channel units along the river continuum. From the model fits for predicting percent STEP height and percent STEEP height I solved for the point along the river continuum where STEEPs exceed STEPs as the dominant unit type contributing to the total elevation of the reach. The switch between STEPs and STEEPs occurs at a basin area of 11.3 km^2. Similarly, the location along the river continuum where FLATs comprise a larger portion of the total elevation than STEPs occurs at 79.4 km^2, but this value occurs outside of the range of basin area observed. However, based on the available data, it is the best estimate of the point along the river continuum where stream reaches would be dominated by a plane bed or pool-riffle pattern, with almost no steps.

These findings allow us to refine our conceptual model for geomorphic control on hyporheic exchange flow in the Lookout Creek Basin. The dominant longitudinal feature driving hyporheic exchange flow in stream reaches with less than 11.3 square kilometers is expected to be steps. Beyond 11.3 square kilometers riffles are expected to be an increasingly dominant longitudinal control on hyporheic exchange flow. However, the influence of steps on hyporheic exchange flow is not expected to be negligible anywhere within the study area.

4.1.3. Idealized profiles

Results show that the general shape of stream longitudinal profiles can be reasonably predicted based on a limited amount of information for basin characteristics, information easily obtained from a map. Of course, some detail is lost when predicting the pattern, size and spacing of channel units with these models. For instance, the homogeneous idealized profiles do not represent sub-unit scale water surface irregularities that were observed in the field. Previous literature on groundwater flow (Tóth, 1962), and hyporheic exchange flow (Baxter and Hauer, 2000), suggests that short flow-path exchange flows, occurring on the spatial scale of large particles, would be nested within larger flow paths occurring at the scale of CSUs or larger. The idealized profiles presented here provide a reasonable estimate of the hydraulic head distribution at this larger scale. The channel unit scale is an appropriate resolution for predicting how patterns in bed form morphology change over the observed portion of the river continuum. However simplified, idealized profiles produced for this study capture, and make available, a basic geomorphic scaling metric.

4.1.4. Summary of observed and expected patterns

Montgomery and Buffington (1997) presented an idealized continuum of channel types ranging in the down-valley direction from cascade to step-pool to plane bed to pool-riffle, and so on. Stream reach types in the Lookout Creek basin are typically cascade or step-pool in the headwaters and step-pool or plane bed in mid-order reaches. Rarely do stream reach types in the study area fall exclusively into one of the above categories. However, the recognition of these reach types provides a framework for summarizing general changes in stream channel morphology observed in this study, and expected patterns in hyporheic exchange flow along the river continuum.

Cascade stream reaches in this study occurred in second order stream reaches, and were heavily influenced by the presence of large boulders, colluvial substrates, the occasional presence of wood, and bedrock outcroppings. Stream longitudinal gradients were steep, and bed profiles were highly irregular. Spacing between bed form features was typically very short, and dictated by the presence of substrate particles that are rarely transported. Occasional channel splits associated with boulders caused steep cross-valley gradients, however, near-stream subsurface flowpaths in these reaches are expected to be primarily in the down-valley direction due to steep longitudinal gradients. In these reach types, high average water surface concavity and short spacing between slope breaks in the stream profiles

indicates a high potential for frequent exchange between the stream and the subsurface.

Step-pool stream reaches were the most common type in this study, occurring in second-, third-, and fourth-order reaches. Steps were most commonly formed by small boulders or other rocky substrates. Wood steps occurred less frequently, and were most common in third order stream reaches. Where wood-caused steps occurred they were taller and steeper than rock-caused steps. Bed topography associated with step-pool sequences in this study showed a higher degree of organization than in cascade reaches. These sequences were characterized by a more or less regular longitudinal pattern of concavities and convexities in the water surface profile. However, portions of step-pool stream reaches were poorly organized and closely resembled either cascade or plane-bed stream reach characteristics. This added variability to the average spacing between slope breaks, which varied from less than a meter to tens of meters. Average water surface concavity was highest where step-pool sequences were well developed, indicating a high potential for gravity driven exchange flow. The magnitude of concavities in the stream profile, and the spacing of bed forms are expected to greatly influence the magnitude of hyporheic exchange flows, the frequency with which water cycles through the hyporheic zone, and the residence time of water in the hyporheic zone. Meander bends were essentially absent, and where stream bends occurred they were typically forced by steep valley walls, colluvial deposits, or debris flow deposits. Subsurface flow paths are not expected to be associated

with meander bends, however width fluctuations in the step-pool pattern may allow for the development of arcuate subsurface flow paths in the alluvium adjacent to the stream (sensu Harvey and Bencala, 1993). The primary mechanism driving exchange flow in step-pool stream reaches is expected to be gravitational exchange associated with bed topography.

Plane-bed channels are characterized by long stretches of relatively featureless bed (Montgomery and Buffington, 1997). Stream reaches characterized as plane-bed in this study were in fourth-order reaches. Average water surface concavity in these reaches was the lowest of any of the alluvial stream reach types, indicating a relatively low potential for gravity driven hyporheic exchange flow in the longitudinal dimension. Subsurface flow paths in these reaches are expected to mostly parallel surface flow paths, except where steep cross-valley gradients exist. Plane-bed reaches in this study were associated with the highest variability in spacing between longitudinal slope breaks indicating that high variability in hyporheic flowpath length is likely. Average hyporheic flow path lengths are expected to be relatively long. In this study, plane bed reach types were associated either with a relatively large amount of bar and channel split development, or none at all. Where bars and channel splits existed, average cross-valley gradients were steep relative to average longitudinal gradient, suggesting that these features may strongly affect exchange flow patterns in plane bed reach types.

No stream reach in this study was classified as pool-riffle, though some pool-riffle sequences did occur in mid-order stream reaches. Pool-riffle channels

are characterized by an undulating bed that defines a sequence of bars, pools, and riffles (Leopold *et al*., 1964, Montgomery and Buffington 1997). Spacing between riffles in pool-riffle reaches is inherently variable, but other studies have shown an average spacing between 5 and 7 channel widths (Knighton, 1984). This suggests that a scaling metric may be available for predicting hyporheic flowpath lengths in these reach types. In this study, the average water surface concavity was relatively lower in reaches where pool-riffle sequences occurred, indicating a lower potential for gravity driven exchange flow in the longitudinal direction.

4.2. WATER SURFACE PROFILES AND HYPORHEIC EXCHANGE FLOW

4.2.1. Applicability of the theoretical model

The theoretical model developed in this study explained approximately 38% of the overall variability observed in the pressure head distribution in the stream bed. The extent to which the pressure distributions within the hyporheic zone of other streams can be explained by the shape of the water surface depends on the physical characteristics of the aquifer, including the cross-sectional area, the shape of the underlying impermeable boundary, heterogeneities in hydraulic conductivity in the bed sediments, and cross-valley hydraulic gradients. The assumptions in the physical model used in this study are rarely met in nature, particularly in highly

irregular mountain streams. However, when studying hyporheic hydrology, some set of assumptions will always be necessary because of the difficulties in measuring the physical properties of the riparian aquifer. The approach used here allowed for quantification of the amount of variability explained by the simplified theoretical model. This allows an informed decision to be made as to whether to accept or reject the assumptions of the model. This study investigated how changes in stream geomorphology can affect patterns in hyporheic exchange flow along the river continuum. Results show that predicting whether a specific location in the stream bed is upwelling or downwelling can be problematic. Results also show that pressure distributions in the stream bed are sufficiently controlled by the shape of the water surface profile to justify comparisons among stream reaches with widely varying morphology. Variations in water surface concavity and slope break size and spacing can be striking, and the theoretical model can be useful for making general predictions in these cases.

4.2.2. Water surface concavity as an indicator for hyporheic exchange flow

Upwelling and downwelling are associated with convexities and concavities in the water surface profile (Vaux, 196; Eq. 2). This study demonstrates that the absolute magnitude of change in pressure gradients along the stream bed is proportional to the magnitude of the concavity in the water surface profile.

Consequently, it can be generally stated that extreme irregularities in the water surface profile are associated with extreme changes in pressure gradients. Because variations in pressure gradients cause hyporheic exchange flow, it follows that a stream reach with a highly irregular longitudinal profile has more potential for gravity-driven hyporheic exchange than a stream reach with a nearly constant slope.

Average water surface concavity (AWSC) is a physically-based, quantifiable metric that can be used as an indicator for comparing the potential for gravity-driven upwelling and downwelling in stream reaches with varying morphology. The physical basis for making these comparisons lies in the inverse relationship between concavity in the water surface profile and the distribution of pressure gradients in the stream bed that influence the vertical motion of water. Researchers can survey longitudinal profiles for different stream reaches, quantify concavities in the water surface profile (by numerically calculating the second derivative of points within the water surface profile) and use AWSC as a quantitative measure of the potential for upwelling and downwelling for the stream reach in general.

This may prove useful for fisheries biologist comparing fish habitat quality. For instance, Geist and Dauble (1998) found that models for predicting habitat quality for chinook salmon (*Onchorynchus tshawytscha*) were improved by incorporating the effects of stream geomorphology on hydraulic processes including hyporheic exchange flow. This study showed specific upwelling zones to

be difficult to predict in small streams, but also demonstrated that the potential for upwelling is influenced by the AWSC, a metric that can be calculated from relatively easily measured channel morphologic metrics, and is predictable based on basin area.

Interest in hyporheic exchange processes has grown, and some researchers have noted the lack of quantifyable metrics available for comparing stream reaches (Bencala, 2000; Findlay, 1995). AWSC provides such a comparative metric. The use of stream tracer studies to investigate hyporheic processes has increased with the development of, and availability of, models to interpret the results of stream tracer tests (Bencala and Walters, 1983; Hart, 1995). Yet linking hyporheic characteristics determined through tracer studies with physical characteristics remains a significant challenge (Harvey *et al*., 1996). AWSC is a metric that relates a physical characteristics of the stream to the distribution of pressure head in the stream bed. This relatively easily measured metric could be useful for linking the results of tracer tests to stream morphology in experiments on stream reaches with varying morphology.

Various research indicates that many factors affect the spatial extent of the hyporheic zone, including saturated hydraulic conductivity, stream discharge, depth of alluvium, catchment wetness, stream geomorphology, and regional groundwater flow (Toth, 1962; Vaux, 1968; Thibideaux and Boyle, 1987; Harvey and Bencala, 1993; Hinton *et al*, 1993; Wondzell and Swanson, 1996b; Wroblicky *et al*., 1998; Baxter and Hauer, 2000). Amongst these factors, the strength of downwelling and

upwelling can be expected to influence the depth to which stream water penetrates the subsurface aquifer. Because the magnitude of pressure gradients are directly influenced by the magnitude of concavity in the stream, the vertical extent of the hyporheic should be affected by AWSC. The results of this study support the prediction that the depth of penetration by stream water into the alluvial aquifer of a gaining stream should increase as ASWC increases. This study also suggests that the amount and frequency of exchange flow should increase as AWSC increases.

The finding that the magnitude of change in pressure gradients increases with the magnitude of concavities underscores the importance of wood and log jams, or any other bed form roughness elements that cause large irregularities in stream longitudinal profiles. I found that wood-caused STEPs were taller and steeper than rock-caused STEPs, indicating that wood-caused STEPs may be more effective at driving hyporheic exchange flow than rock-caused STEPs. The relationship between concavity in the water surface profile and the potential for vertical motion of water through the stream bed provides a physical explanation for the beneficial effect of wood on hyporheic exchange flow. Where wood in rivers increases AWSC, the potential for hyporheic exchage flow is also increased.

For those intending to use AWSC as a metric, it will be helpful to consider various techniques for numerical differentiation and their limitations. Simpler formulas for numerical integration are available than the one used in this study (Charpa, 1988). This study required the use of a technique for derivation of unequally spaced data because piezometer installation was difficult. Equally

spaced survey data would allow for simpler calculation of ASWC. Obtaining the best results using AWSC as a metric will require highly accurate survey data.

4.2.3. Dominant mechanisms driving hyporheic exchange flow

Research on convective transport of water and solutes through bed forms (Savant *et al*., 1987; Thibodeaux and Boyle, 1987; Packman and Brooks 2001) shows that pressure gradients set up by water flowing over dune-like bed forms drive convective subsurface exchange flow in laboratory flumes (the pumping model). The conceptual model I tested does not account for this mechanism. Instead, I focused entirely on gravity-driven exchange flow caused by the distribution of elevation gradients in the water surface profile. While this may seem at odds with other research, the present study occurred in streams where elevation gradients are a more striking characteristic than velocity gradients. Results and observations from this study suggest that steep slope breaks in the water surface profile are the dominant control on hyporheic exchange in headwater streams.

Headwater streams are characterized by highly irregular beds with poorly sorted bed substrates that cause chaotic and turbulent stream flow. Average water velocity, measured on 6/9/02, increased from less than 0.16 ms^{-1} in the second-order main stem Lookout Creek to about 0.7 ms^{-1} in the fourth-order main stem

(Gooseff, unpublished tracer test data), indicating that velocity increases along the river continuum. Average water surface concavity (AWSC) in headwater streams in this study decreased with increasing drainage basin area, suggesting that gravity-driven exchange flow is an especially important mechanism in headwater cascade and step-pool stream reach types, and less important farther downstream where water surface profiles are smoother. The observed increase in stream water velocity along the river continuum suggests that the importance of velocity-driven convective exchange flow may increase with stream size, however, this has not been tested. To date, I know of no study that has examined the relative importance of gravity-driven versus velocity-driven exchange flow in real streams.

4.3. HYPORHEIC EXCHANGE IN THE RIVER CONTINUUM

4.3.1. Spacing of upwelling and downwelling zones

Results indicate that the shape of the water surface profile influences the location of upwelling and downwelling zones in the study reaches, and that the spacing between slopes breaks in stream water surface profiles increases predictably throughout the study area. A synthesis of these results supports the general hypothesis that hyporheic flow path lengths are scaled to bed forms and increase accordingly along the river continuum. As the spacing between slope

breaks in the water surface profile increases, the spacing between transition points from downwelling to upwelling are also expected to increase, thus decreasing the frequency of exchange between the stream and the hyporheic zone. Further support is provided by the comparison of downwelling zone lengths in different size streams, which also showed that downwelling zones increase with increasing basin area.

The rate of the increase in downwelling zone length also suggests that a geomorphic scaling metric can be a useful indicator of changes in average hyporheic flow path lengths. The piezometer transects are in reaches with contributing areas of 1.98 km^2 and 16.87 km^2. Over this range, the slopes of the trend lines are 0.32 for FLAT lengths and 0.39 for downwelling zone lengths, suggesting that the length of FLATs and the length of downwelling zones increase at a similar rate. The length of FLAT CSUs are predicted to increase from 2.05 m to 7.82 m over this range in basin areas, and downwelling zone lengths are predicted to increase from 3.28 m to 8.02 m.

I observed more downwelling than upwelling in piezometer transects. Where upwelling did occur it was typically just downstream from STEPs or within STEEPs (figures 13, 14, and 15). Analysis of the relative abundance of CSUs showed that the percentage of reach length in FLATs increased while the percentage of reach length in STEEPs and STEPs decreased along the river continuum. This suggests that the relative abundance of upwelling zones should decrease along the river continuum.

All of the above evidence supports the general hypothesis that hyporheic flowpath lengths are scaled to bed forms, the lengths of which increase from headwater to mid-order streams. Where slope breaks are frequent, such as in headwater streams, I predict that water will cycle through the hyporheic zone frequently, along short flow paths. In mid-order streams where slope breaks are less frequent, I predict that water will exchange less frequently, along longer flowpaths. Because repeated interchange increases the extent of contact and contact time with geochemically and microbially active sediment (Harvey and Wagner, 2000), more frequent exchange is expected to increase processing rates of organic matter and nutrients. Frequent hydrologic exchange is also expected to increase the exchange of heat between the stream and the hyporheic zone, and increase the retention of water, effectively moderating temperatures and discharge rates.

This study covered only a small portion of the river continuum in channels where steps were usually present. Predictions outside the observed range in basin area are only speculative, still, evidence supporting bed form scaling of hyporheic flow paths suggests that geomorphic scaling metrics may be appropriate in other bed-form configurations, and elsewhere within the river continuum. Geomorphologists have identified more or less periodic bed form spacing in pool-riffle, dune, and ripple bed forms (Knighton, 1984). These morphologies may present useful scaling metrics. Other researchers have noted that hyporheic exchange flow is controlled at varying scales, and have noted the importance of

scale in determining the functional significance of hyporheic exchange flow (Boulton *et al*., 1998). Bed-form spacing within the river continuum may present untapped opportunities for understanding the link between channel form and ecological function in streams and rivers.

4.3.2. Hyporheic residence times

Hyporheic exchange flow occurs over a wide range of time scales influenced by channel morphologic features (Haggerty *et al*., 2002). The time scale for water flowing through the hyporheic zone is influenced by the hydraulic conductivity of the subsurface aquifer, the hydraulic gradient, and the length of the flowpath. My results suggest that mean longitudinal hyporheic flowpath lengths will increase, and that hydraulic gradients will decrease along the river continuum. Each of these longitudinal trends would lead to an increase in mean hyporheic residence time with increasing basin area. Hydraulic conductivity was not measured in this study, however Kasahara (2000) reported an increase in hydraulic conductivity from a second-order tributary of Lookout Creek, to the main stem. This trend could be expected to somewhat offset the effects of the observed trends in increasing length and decreasing hydraulic gradients on hyporheic residence times. Further research on the residence time distributions of hyporheic water in different stream reaches may provide more insight into the net effects of increases in bed form spacing and downwelling zone lengths along the river continuum.

4.3.4. The context of valley morphology

In stream systems draining glaciated terrain, such as in the Flathead River Valley, MT, USA and the Swan River Valley, MT, USA, studies have indicated that valley geomorphology and the presence of alluvial valley segments bounded by knick points offer a framework for predicting reach-scale downwelling and upwelling, a finding that has helped shape the Hyporheic Corridor Concept (Stanford and Ward, 1993; Baxter and Hauer, 2000). The concept represents one conceptual model for hyporheic exchange flow within the river continuum. Baxter and Hauer (2000) showed that average VHGs were consistently negative at the upstream end, neutral in the middle of, and positive at the downstream end of bounded alluvial valley segments. Despite this valley-segment scale geomorphic influence, Baxter and Hauer (2000) commonly observed upwelling and downwelling occurring at the channel-unit scale, just upstream from valley-constraining geologic knick points. This suggests that the shape of the water surface profile can still be a good general predictor of patterns of upwelling and downwelling, even when the cross-sectional area of the aquifer is not constant. Furthermore, patterns in upwelling and downwelling may be more responsive to channel-unit scale morphologic features, than to the valley-scale morphology in other geologic settings (Baxter and Hauer, 2000). In some cases, strong reach-scale patterns in upwelling or downwelling may not exist, even where bounded alluvial valley segments exist. In contrast to the results from the Flathead valley studies, a

study conducted in the Middle Fork John Day River in northeast Oregon, Wright *et al* (in review) found little evidence for reach-scale upwelling and downwelling in association with valley geomorphology.

Bounded, alluvial-valley segments such as those observed in glaciated landscapes may be less common elsewhere. Only one out of twelve of the randomly selected stream reaches in the Lookout Creek Basin occurs in a geologic setting that fits the description of a bounded alluvial-valley segment. All other reaches occurred in unbounded or at best, weakly bounded alluvial-valley segments. Though the influence of valley morphology on reach-scale patterns in upwelling and downwelling cannot be ignored, I expect that morphologic features at the channel-unit scale will offer more explanatory power than valley morphology in predicting patterns in upwelling and downwelling in headwater streams and mid-order streams. This prediction is consistent with the results of Kasahara and Wondzell (in press).

Despite difficulties in demonstrating valley-scale patterns in hyporheic exchange flow, the Hyporeic Corridor Concept offers a useful conceptual framework for the control hyporheic exchange flow by valley morphology in the river continuum. The present study offers a framework for the control of hyporheic exchange flow by stream bed morphology within the river continuum. The two conceptual models are by no means exclusive.

5. CONCLUSIONS

Changes in the size, spacing, and character of slope breaks in stream water surface profiles are predictable based on drainage basin area and stream reach gradient. The spacing between slope breaks increases, and the size of steps decreases with increasing drainage basin area. Models incorporating distances between slope breaks as a scaling metric can be used to make reasonable predictions for the shape of the water surface profile at different points along the river continuum. The idealized profiles produced for this study are highly simplified, but the level of resolution is appropriate for predicting bed form morphologic changes that occur from the headwaters to the mouth of a fourth-order mountain stream drainage basin. Bed form spacing provides a scaling metric that is a useful indicator for the average length of upwelling and downwelling zones in stream beds.

Predicting the exact location and frequency of upwelling and downwelling zones from the shapes of water surface profiles in this study was not possible. However, results demonstated that the magnitude of variations in pressure gradients in the stream bed was controlled by the magnitude of variations in concavity in water surface profiles. I conclude that the potential for hyporheic exchange flow in stream reaches increases as the magnitude of concavities and convexities in the water surface profile increases. I've shown that numerical techniques for

differentiation can be used to quantify average water surface concavity (AWSC), and I suggest that stream researchers can refine their studies of hyporheic exchange flow by quantifying and reporting AWSC as a metric for predicting the potential for gravity driven hyporheic exchange flow in stream reaches. Furthermore, AWSC is easily predictable from basin area, indicating that the behavior of pressure gradients in the hyporheic zone changes predictably along the river continuum.

It is unlikely that there is any single readily measurable physical property that explains more variability in patterns of upwelling and downwelling in small to mid-order mountain streams than the shape of the water surface profile. In these streams, irregularities in the longitudinal profiles are associated with very steep hydraulic gradients that cause hyporheic exchange flow. I suggest that gravity-driven pressure gradients are the dominant mechanism driving exchange flow in steep headwater streams with highly irregular longitudinal profiles.

Increases in bed form spacing along the river continuum have the potential to affect the frequency with which water cycles through stream bed sediments, the mean hyporheic flowpath length, and the mean residence time distribution of water and solutes in the hyporheic zone. This in turn can affect the retention of water and solutes, the rate of organic matter processing, the rate and nature of nutrient transformations, the rate of heat exchange between the stream and the subsurface, and the type of habitat provided in the hyporheic zone. Finally, I conclude that a

river continuum model is an appropriate framework for predicting the effects of bed form morphology on hyporheic exchange flow.

BIBLIOGRAPHY

Baxter CV, Hauer FR. 2000. Geomorphology, hyporheic exchange, and selection of spawning habitat by bull trout (Salvelinus confluentus). *Canadian Journal of Fisheries and Aquatic Science* **57**:1470-1481.

Bencala KE. 2000. Hyporheic zone hydrological processes. *Hydrological Processes* **14**: 2797-2798.

Bencala KE, Walters RA. 1983. Simulation of solute transport in a mountain pool-and-riffle Stream: A transient storage model. *Water Resources Research* **19**: 718-724.

Bierlmaier FA, McKee A. 1989. Climatic summaries and documentation for the primary meteorological station, H.J. Andrews Experimental Forest, 1972 to 1984, U.S. Dep. Of Agric. For. Serv., Portland OR.

Boulton AJ, Findlay S, Marmonier P, Stanley E H, Valett HM. 1998. The functional significance of the hyporheic zone in streams and rivers. *Annual Review of Ecology and Systematics* **29**: 59-81.

Brunke M, Gonser T. 1997. The ecological significance of exchange processes between rivers and groundwater. *Freshwater Biology* **37**: 1-33.

Charpa SC. 1988. *Numerical Methods for Engineers*. McGraw-Hill: USA.

Curry RA, Noakes DLG. 1995. Groundwater and selection of spawning sites by brook trout (Salvelinus fontanalis). *Canadian Journal of Fisheries and Aquatic Sciences* **52**: 1733-1740.

Dahm CN, Vallett HM. 1996. Hyporheic zones. In *Methods in Stream Ecology*, Hauer FR, Lamberti GA (eds). Academic Press: San Diego; 107-119.

Findlay S. 1995. Importance of surface-subsurface exchange in stream ecosystems: The hyporheic zone. *Limnology and Oceanography* **40(1)**: 159-164.

Geist DR, Dauble DD. 1998. Redd site selection and spawning habitat use by fall chinook salmon: the importance of geomorphic features in large rivers. *Environmental Management* **22(5)**: 655-669.

Grant GE, Swanson FJ. 1995. Morphology and processes of valley floors in mountain streams, western Cascades, Oregon. Geophysical monograph 89. USDA Forest Service, Pacific Northwest Research Station. Corvallis, OR.

Grant GE, Swanson FJ. Wolman MG. 1990. Pattern and origin of stepped-bed morphology in high-gradient streams, Western Cascades, Oregon. *Geological Society of America Bulletin* **102**: 340-352.

Haggerty R, Wondzell SM, Johnson MA. 2002. Power-law residence time distribution in the hyporheic zone of a 2nd-order mountain stream. *Geophysical Research Letters* **29(13)**: 18.1-18.4.

Hart DR. 1995. Parameter estimation and stochastic interpretation of the transient storage model for solute transport in streams. *Water Resources Research* **31(2)**: 323-328.

Harvey JW, Bencala KE. 1993. The effect of streambed topography on surface-subsurface water exchange in mountain catchments. *Water Resources Research* **29(1)**:89-98.

Harvey JW, Wagner B J. 2000. Quantifying hydrologic interactions between streams and their subsurface hyporheic zones. In *Streams and Ground Waters*. J. A. Jones and P. J. Mulholland (eds). Academic Press: San Diego; 3-44.

Harvey JW, Wagner BJ, Bencala KE. 1996. Evaluating the reliability of the stream tracer approach to characterize stream-subsurface water exchange. *Water Resources Research* **32**: 2241-2451.

Hill AR, Labadia CF, Sanmugadas K. 1998. Hyporheic zone hydrology and nitrate dynamics in relation to the streambed topography of a N-rich stream. *Biogeochemistry* **42**: 285-310

Hinton MJ, Schiff SL, English MC. 1993. Physical properties governing groundwater flow in a glacial till catchment. *Journal of Hydrology* **142**: 229-249.

Kasahara T. 2000. Geomorphic controls on hyproheic exchange flow in mountain streams. MS. Thesis, Oregon State University. 103 p.

Kasahara T. Wondzell SM. in press. Geomorphic controls on hyporheic exchange flow in mountain streams. *Water Resources Research*

Keller EA. 1978. Pools, riffles, and channelization. *Environmental Geology* **2**: 119-127.

Keller EA, Melhorn WN. 1973. Bedforms and fluvial processes in alluvial stream channels: selected observations. In, *Fluvial Geomorphology*, Morisawa M (ed). New York State University Publications in Geomorphology: Bringhamton; 253-283.

Keller EA, Melhorn WN. 1978. Rhythmic spacing and origin of pools and riffles. Bulletin of the *Geological Society of America* **89**: 723-730.

Knighton D. 1984. *Fluvial Forms and Processes*. Edward Arnold Ltd: London; 218.

Leopold LB, Wolman MF, Miller JP. 1964: *Fluvial Processes in Geomorphology*. WH Freeman; San Francisco.

Lenzi MA. 2001. Step–pool evolution in the Rio Cordon, northeastern Italy. *Earth Surface Processes and Landforms* **26**: 991-1008.

McDonald MG, Harbaugh AW. 1984. A modular three-dimensional finite-difference groundwater flow model. *U.S. Geological Survey Open File Report 83*.

Malard F, Mangin A, Uehlinger U, Ward JV. 2001. Thermal heterogeneity in the hyporheic zone of a glacial floodplain. *Canadian Journal of Fisheries and Aquatic Sciences* **58**: 1319-1335.

Montgomery DR, Buffington JM. 1997. Channel-reach morphology in mountain drainage basins. *Geological Society of America Bulletin*; **109(5)**: 596-611.

Montgomery D, Buffington JM, Peterson NP, Schuett-Hames D, Quinn TP. 1996. Stream bed scour, egg burial depths, and the influence of salmonid spawning on bed surface mobility and embryo survival. *Canadian Journal of Fisheries and Aquatic Science* **53**: 1061–1070.

Morrice JA, Valett HM, Dahm CN, Campana ME. 1997. Alluvial characteristics, groundwater-surface water exchange and hydrological retention in headwater streams. *Hydrological processes* **11**: 253-267.

Orghidan T. 1959. Ein neuer Lebensraum des unterirdischen Wassers: der hypoheische Biotop. *Archives of Hydrobiology* **55**:392-414

Packman AI, Brooks NH. 2001. Hyporheic exchange of solutes and colloids with moving bed forms. *Water Resources Research* **37(10)**: 2591-2605.

Ramsey FL, Schafer DW. 1997. *The Statistical Sleuth: a course in methods of data analysis*. Wadsworth pubishing Company: Belmont; 742.

Richards KS. The morphology of riffle-pool sequences. 1976. *Earth Surface Processes* **1**: 71-88.

Runkel RL. 1988. One-dimensional transport with inflow and storage (OTIS): A solute transport model for streams and rivers. *US Geological Survey, Water-Resources Investigation Report 98-4018*, Denver, Colorado.

Savant SA, Reible DD, Thibodeaux LJ. 1987. Convective transport within stable river sediments. *Water Resources Research* **23**: 1763-1768.

Schumm, SA. 1977. *The Fluvial System*. John Wiley and Sons: New York.

Stanford JA, Ward JV. 1988. The hyporheic habitat of river ecosystems. *Nature* **335**: 64-66

Stanford JA, Ward JV. 1993. An ecosystem perspective of alluvial rivers: connectivity and the hyporheic corridor. *Journal of the North American Benthological Society*: **12(1)**: 48-60.

Strahler AN. 1964. Quantitative geomorphology of drainage basins and channel networks. In *Handbook of Applied Hydrology*,Ven te Chow (ed). McGraw-Hill: New York.

Thibodeaux LJ, Boyle JD. 1987. Bedform-generated convective transport in bottom sediment. *Nature* **325**:341-343.

Toth. J. 1962. A theory of groundwater motion in small drainage basins in central Alberta Canada. Journal of Geophysical Research **67**:4375-4387.

Torgensen CE, Price DM, Li HW, McIntosh BA. 1999. Multiscale thermal refugia and stream habitat associations of Chinook salmon in northeastern Oregon. *Ecological Applications* **9(1)**: 301-319.

Triska FJ, Kennedy VC, Avanzio RJ, Zellweger GW, Bencala KE. 1989. Retention and transport of nutrients in a third-order stream in northwestern California: Hyporheic processes. *Ecology* **70**: 1893-1905.

Vannote RL, Minshall GW, Cummins KW, Sedell JR, Cushing CE. 1980. The river continuum concept. *Canadian Journal of Fisheries and Aquatic Sciences* **37**: 130-137.

Vaux WG. 1968. Intragravel flow and interchange of water in a streambed. *USDI, US Fish and Wildlife Service, Fishery Bulletin* **66(3)**: 479-489.

Valett HM. 1993. Surface-hyporheic interactions in a Sonoran Desert stream: Hydrologic exchange and diel periodicity. *Hydrobiologia* **259**: 133-144.

Valett HM, Fisher SG, Grimm NB, Camill P. 1994. Vertical hydrologic exchange and ecological stability of a desert stream ecosystem. *Ecology* **75**: 548-560.

White DS. 1993. Perspectives on defining and delineating hyporheic zones. *Journal of the North American Benthological Society* **12**:61-69.

White DS, Elzinga CH, Hendricks SP. 1987. Temperature patterns within the hyporheic zone of a northern Michigan river. *Journal of the North American Benthological Society* **6**: 85-91.

Wondzell SM, Swanson FJ. 1996a. Seasonal and storm dynamics of the hyporheic zone of a 4th-order mountain stream II: Nitrogen cycling. *Journal of the North American Benthological Society* **15(1)**: 20-34.

Wondzell SM, Swanson FJ. 1996b. Seasonal and storm dynamics of the hyporheic zone of a 4th-order mountain stream I: Hydrological processes. *Journal of the North American Benthological Society* **15(1)**: 3-19.

Wright KK, Baxter CV, Li JL. in review. A search for hyporheic upwelling and ecological responses in an arid montane alluvial river. *Journal of Freshwater Biology*.

Wroblicky GJ, Campana ME, Valett HM, Dahm CN. 1998. Seasonal variation in surface-subsurface water exchange and lateral hyporheic area of two stream-aquifer systems. *Water Resources Research* **34**: 317-328.